

UNCLASSIFIED

AD NUMBER: AD0815377

LIMITATION CHANGES

TO:

Approved for public release; distribution is unlimited.

FROM:

Further dissemination only as directed by Army Materiel Command, Redstone Arsenal, AL, 35809; 1 Jan 1967; or higher DoD authority.

AUTHORITY

USASAC ltr dtd 2 May 1974

AD81537  
FILE COPY

Final Report

# APPLICATION OF THE EXTENDED KALMAN FILTER TO BALLISTIC TRAJECTORY ESTIMATION

By: R. E. LARSON R. M. DRESSLER R. S. RATNER

Prepared for:

NIKE-X PROJECT OFFICE  
U.S. ARMY MATERIEL COMMAND  
REDSTONE ARSENAL, ALABAMA

DDC  
RECEIVED  
JUN 9 1967  
RECEIVED  
BC

CONTRACT DA-01-021-AMC-90006(Y)

STANFORD RESEARCH INSTITUTE

MENLO PARK, CALIFORNIA





11) January 1967

12) 53p.

9) Final Report, 1 Oct 65 - 30 Sep 66

6) APPLICATION OF THE EXTENDED KALMAN FILTER TO BALLISTIC TRAJECTORY ESTIMATION.

10) Robert E. LARSON, Robert M. DRESSLER, Robert S. RATNER

Prepared for:

NIKE-X PROJECT OFFICE  
U.S. ARMY MATERIEL COMMAND  
REDSTONE ARSENAL, ALABAMA

15)

CONTRACT DA-01-021-AMC-90006(Y)

16) SRI-5188-103

Approved: PHILIP E. MERRITT, MANAGER  
INFORMATION AND CONTROL LABORATORY

JERRE D. NOE, EXECUTIVE DIRECTOR  
ENGINEERING SCIENCES AND INDUSTRIAL DEVELOPMENT

Copy No. 136

esd/

STATEMENT #5 UNCLASSIFIED

mlh

This document may be further distributed by any holder only with specific prior approval of Army Materiel Command  
attn: AMC PM - NXR - E,  
Redstone Arsenal, Ala

## ABSTRACT

---

In this report an extended Kalman filter for ballistic trajectory estimation is presented. The filter equations are basically the same as those in the previous Final Report on this contract. The several modifications are explained in detail, and values for all filter parameters are given. The filter was tested against simulated radar data for a number of different cases; performance was excellent in all cases. For comparison purposes a second-order exponentially weighted polynomial filter was used on the same data; the performance was significantly worse than for the extended Kalman filter. The extended Kalman filter was also run at slower data rates and with multiple interruptions of data with only a slight degradation in performance. A precomputed approximation to the weighting matrix was calculated on the basis of several runs; this approximation performed nearly as well as the fully implemented filter. Use of this approximation reduced computational requirements by an order of magnitude.

## CONTENTS

---

ABSTRACT . . . . .	ii
LIST OF ILLUSTRATIONS . . . . .	iv
LIST OF TABLES . . . . .	iv
I INTRODUCTION . . . . .	1
II FILTER EQUATIONS . . . . .	3
A. The Linear-Gaussian Case . . . . .	3
B. The Extended Kalman Filter . . . . .	4
III EQUATIONS FOR ESTIMATION OF A BALLISTIC TRAJECTORY . . . . .	7
A. Equations of Motion . . . . .	7
B. Observation Equations . . . . .	10
IV NUMERICAL RESULTS FOR THE EXTENDED KALMAN FILTER . . . . .	15
V COMPARISON WITH POLYNOMIAL FILTERS . . . . .	25
A. Qualitative Comparison . . . . .	25
B. Comparison with the Exponentially Weighted Polynomial Filter . . . . .	25
VI EFFECTS OF VARIATION IN DATA RATE AND DATA INTERRUPTION . . . . .	32
A. Variation in Data Rate . . . . .	32
B. Data Interruption. . . . .	32
VII PRECOMPUTATION OF THE WEIGHTING MATRIX . . . . .	40
A. Computational Requirements of the Extended Kalman Filter . . . . .	40
B. Use of a Precomputed Weighting Matrix . . . . .	40
C. Experimental Results Using a Precomputed Weighting Matrix . . . . .	41
VIII CONCLUSIONS AND RECOMMENDATIONS FOR FUTURE STUDY . . . . .	45
REFERENCES . . . . .	47

## ILLUSTRATIONS

---

Fig. 1 Radar Face Coordinates . . . . .	12
Fig. 2 Relation of Radar Face Coordinates to Ground Coordinates . . . . .	12
Fig. 3 Test Trajectories . . . . .	16
Fig. 4 Measurement Noise . . . . .	20
Fig. 5 Extended Kalman Filter—Case 1 . . . . .	21
Fig. 6 Extended Kalman Filter—Case 2 . . . . .	22
Fig. 7 Extended Kalman Filter—Case 3 . . . . .	23
Fig. 8 Extended Kalman Filter—Case 4 . . . . .	24
Fig. 9 Polynomial Filter—Case 1 . . . . .	28
Fig. 10 Polynomial Filter—Case 2 . . . . .	29
Fig. 11 Polynomial Filter—Case 3 . . . . .	30
Fig. 12 Polynomial Filter—Case 4 . . . . .	31
Fig. 13 Extended Kalman Filter—Case 1, $\Delta t = 0.10$ sec. . . . .	33
Fig. 14 Extended Kalman Filter—Case 1, $\Delta t = 0.25$ sec. . . . .	34
Fig. 15 Extended Kalman Filter—Case 4, $\Delta t = 0.10$ sec. . . . .	35
Fig. 16 Extended Kalman Filter—Case 4, $\Delta t = 0.25$ sec. . . . .	36
Fig. 17 Effect of Data Interruption on Extended Kalman Filter—Case 1 . . . . .	37
Fig. 18 Effect of Data Interruption on Extended Kalman Filter—Case 4 . . . . .	38
Fig. 19 Precomputed Filter—Case 1 . . . . .	43
Fig. 20 Precomputed Filter—Case 4 . . . . .	44

## TABLES

Table 1 Initial Conditions . . . . .	17
--------------------------------------	----

## I INTRODUCTION

One of the major tasks performed by the Control Systems Laboratory in support of NIKE-X System Evaluation Studies during 1966 was the final design and testing of an extended Kalman filter for estimation of ballistic trajectories. The purpose of this report is to summarize the filter design and to present numerical results for a number of examples.

The basic theory of the extended Kalman filter was covered in last year's final report.<sup>1\*</sup> A brief review of this material appears in Sec. II.

A complete specification of a computer program to implement the filter also was given in last year's report.<sup>1</sup> However, in order to obtain improved filter performance, a few modifications of the basic equations were made. The most notable change is in the way in which  $\beta$ , the ballistic coefficient, is estimated; the quantity  $\rho/\beta$ , where  $\rho$  is atmospheric density, is estimated directly by the filter, instead of  $\beta_0$  and  $\beta_1$ , the coefficients in the expression  $\beta = \beta_0 + \beta_1 z$ , where  $z$  is altitude. Complete filter equations, including all modifications, appear in Sec. III.

An important aspect of the design procedure is the so-called "final tuning." This process consists of determining values for  $S(0/-1)$ , the covariance matrix of the initial estimate, and  $Q(k)$ , the covariance matrix of the random forcing function. These values can be determined to within an order of magnitude by physical considerations, but further adjustment is generally necessary to achieve the best filter performance. Adjustment of  $S(0/-1)$  controls the transient response, while adjustment of  $Q(k)$  affects the steady-state performance. The final values chosen for these matrices are given in Sec. IV.

The filter was tested and evaluated by giving it noisy measurements of an actual trajectory and comparing its estimates with the true values. The actual trajectories were obtained from a detailed simulation of a ballistic re-entry vehicle,<sup>2</sup> while the measurement noise was generated using a radar model based on work by Bell Telephone Laboratories.<sup>3</sup> The performance of a particular filter design was evaluated on the basis of how well the estimated values compared with the true values. Estimation

---

\* References are listed at the end of the report.

errors in position, velocity, acceleration, and the actual and estimated  $\beta$  were plotted as a function of time for all runs. These error plots were then analyzed on the basis of time for initial transient to die out, maximum error, and steady-state error. The performance of the final filter in terms of these criteria was excellent. A representative set of plots is included in Sec. IV.

For purposes of comparison the exponentially weighted filter described in the previous final report<sup>1</sup> was tested with the same input as for the extended Kalman filter. As was to be expected, the performance of the extended Kalman filter was considerably better. A summary of this comparison, as well as a qualitative comparison of the extended Kalman filter with other polynomial filters is included in Sec. V.

In addition to the standard test runs, a number of other experiments were conducted with the filter. These included variation of the data rate and suppression of data for certain intervals. The filter performance was only slightly degraded when the data rate was reduced from 20 to 4 measurements per second. Multiple data interruptions of 1 second had a negligible effect, once data input was resumed. These experiments are discussed in Sec. VI.

Because of the impressive performance of the extended Kalman filter, it is interesting to consider the possibility of real-time implementation. The computational requirements of the filter are discussed in Sec. VII, and it is shown that real-time implementation of the filter as specified in this report is a difficult but feasible task for current computers. However, it is possible to precompute the weighting matrix,  $W(k)$ , with the result that both storage and computation time requirements can be vastly reduced. This approach was tried on a number of cases, with the result that computing time was reduced by a factor of 30 with only a slight degradation in filter performance. A detailed discussion of this approach and its results is given in Sec. VII.

The last section of the report summarizes the results of this study and indicates future extensions.

## II FILTER EQUATIONS

### A. The Linear-Gaussian Case

The Kalman Filter equations specify an estimate of the state of a linear time-varying dynamical system observed sequentially in the presence of additive white Gaussian noise.<sup>4</sup> The estimate obtained at each time is the maximum-likelihood estimate conditioned on all observations made up to that time. The vector difference equation

$$\underline{x}(k+1) = \Phi(k)\underline{x}(k) + \Gamma(k)\underline{w}(k) \quad (1)$$

describes such a system, where the components of  $\underline{x}(k)$  are the states of the system; and  $\underline{w}(k)$  is a white Gaussian noise process that may represent either actual input noise or inaccuracies in the system model. At each instant of time, observations represented by the vector  $\underline{z}(k)$  are made according to

$$\underline{z}(k) = H(k)\underline{x}(k) + \underline{v}(k) \quad (2)$$

where  $\underline{v}(k)$  is a white Gaussian noise process assumed independent of  $\underline{w}(k)$ . The covariances of  $\underline{w}(k)$  and  $\underline{v}(k)$  are denoted  $Q(k)$  and  $R(k)$  respectively, and it is assumed that an *a priori* estimate  $\hat{\underline{x}}(0/-1)$  has been made with error covariance  $S(0/-1)$ . Here and throughout this report  $\hat{\underline{x}}(i/j)$  will denote the estimate of the state  $\underline{x}$  at time  $i$ , given observations through time  $j$ , and  $S(i/j)$  will denote the covariance of the error in this estimate. The filtering equations may be written<sup>1</sup> as a set of *prediction equations*:

$$\hat{\underline{x}}(k/k-1) = \Phi(k-1)\hat{\underline{x}}(k-1/k-1) \quad (3)$$

$$S(k/k-1) = \Phi(k-1)S(k-1/k-1)\Phi^T(k-1) + \Gamma(k-1)Q(k-1)\Gamma^T(k-1) \quad (4)$$

which describe the behavior of the estimate and its error covariance at time  $k$  on the basis of knowledge of the observations through time  $k-1$ , and a set of *correction equations*:

$$\hat{\underline{x}}(k/k) = \hat{\underline{x}}(k/k-1) + W(k)[\underline{z}(k) - H(k)\hat{\underline{x}}(k/k-1)] \quad (5)$$

$$W(k) = S(k/k-1)H^T(k)[R(k) + H(k)S(k/k-1)H^T(k)]^{-1} \quad (6)$$

$$S(k/k) = [I - W(k)H(k)]S(k/k-1) \quad (7)$$

which take into account the last observation  $\underline{z}(k)$ . The *a priori* estimate and error covariance are used as initial conditions for these recursive relations.

### B. The Extended Kalman Filter

For the case of estimating the state of a ballistic re-entry vehicle on the basis of noisy measurements, the Kalman theory cannot be applied directly because the system equations governing the vehicle are nonlinear. In Appendix E of Ref. 1 the theory is applied to the nonlinear case by using the form of the equations of the Kalman filter and making appropriate linearizations. To obtain a linear observation equation, the nonlinear observation is linearized at each instant  $k$  about the predicted estimate  $\hat{\underline{x}}(k/k-1)$ . The nonlinear observation equation is written as

$$\underline{z}'(k) = \underline{h}[\underline{x}(k)] + \underline{v}'(k) \quad (8)$$

where  $\underline{z}'$  and  $\underline{x}$  have dimension  $m$  and  $n$  respectively, with  $m \leq n$ , and  $\underline{h}$  is an  $m$ -dimensional vector function. The covariance of the zero mean noise  $\underline{v}'$  is denoted  $R'(k)$ . In the present case the  $m$  components of  $\underline{z}'$  are linearly independent functions of the first  $m$  components of the state  $\underline{x}$ , so it is possible to define the nonsingular  $m \times m$  matrix  $T(\underline{x})$  as

$$T(\underline{x}) = \begin{bmatrix} \frac{\partial h_1(\underline{x})}{\partial x_1} & \dots & \frac{\partial h_1(\underline{x})}{\partial x_m} \\ \vdots & & \vdots \\ \frac{\partial h_m(\underline{x})}{\partial x_1} & \dots & \frac{\partial h_m(\underline{x})}{\partial x_m} \end{bmatrix}^{-1} \quad (9)$$

For simplicity in implementing the filter equations it is convenient to consider the measurement vector to be

$$\underline{z}(k) = T(\underline{x})\underline{z}'(k) \quad (10)$$

rather than  $\underline{z}'(k)$ . Since  $T$  is nonsingular this procedure is merely a coordinate transformation. In this case the linearized observation equation becomes<sup>1</sup>

$$z(k) = H\underline{x}(k) + \underline{v}(k) \quad (11)$$

where  $H$  is an  $m \times n$  matrix with elements

$$H_{i,j} = \begin{cases} 1 & , \quad i = j \\ 0 & , \quad i \neq j \end{cases} \quad (12)$$

and  $\underline{v}(k)$  is a zero mean noise with covariance

$$R(k) = T(\underline{x})R'(k)T^T(\underline{x}) \quad (13)$$

The three correction equations, Eqs. (5), (6), and (7), are now specified.

The prediction equation for the state estimate is obtained by directly integrating the nonlinear system equation. If the nonlinear continuous-time system equation is

$$\dot{\underline{x}}(t) = \underline{f}[\underline{x}(t)] + \underline{G}\underline{w}(t) \quad (14)$$

the prediction equation, Eq. (3), can be written as

$$\hat{\underline{x}}(k/k - 1) = \hat{\underline{x}}(k - 1/k - 1) + \underline{f}[\hat{\underline{x}}(k - 1/k - 1)]\Delta t \quad (15)$$

where  $\Delta t$  is the time interval between observations. Since  $\underline{w}$  is a zero mean process, the terms involving it become zero when the expectation is taken.

To update the covariance a linear transition matrix  $\Phi(k)$  is required. This is obtained in Appendix E of Ref. 1 as

$$\Phi(k) = I + F[\hat{\underline{x}}(k/k)]\Delta t \quad (16)$$

where  $F$  is the  $n \times n$  matrix with components

$$F_{ij}(\underline{x}) = \frac{\partial f_i(\underline{x})}{\partial x_j} \quad (17)$$

The distribution matrix  $\Gamma$  is obtained from the continuous-time equation, Eq. (14), as<sup>1</sup>

$$\Gamma = G\Delta t \quad (18)$$

Equations (15), (4), (5), (6), and (7) together with definitions (9), (13), (16), (17), and (18) constitute the extended Kalman filter as specified in Appendix E of Ref. 1. An *a priori* estimate and its error covariance are used as initial conditions for computation.

### III EQUATIONS FOR ESTIMATION OF A BALLISTIC TRAJECTORY

#### A. Equations of Motion

The equations of motion for the present ballistic re-entry problem are taken to be<sup>1</sup>

$$\begin{aligned}\ddot{x} &= \frac{-\rho g V \dot{x}}{2\beta} \\ \ddot{y} &= \frac{-\rho g V \dot{y}}{2\beta} \\ \ddot{z} &= \frac{-\rho g V \dot{z}}{2\beta} - g \quad , \quad (19)\end{aligned}$$

where  $x$ ,  $y$ ,  $z$  are the radar-centered cartesian coordinates of the target vehicle, and

$$\begin{aligned}g &= \text{Gravitational acceleration} \\ \beta &= \text{Ballistic parameter} \\ \rho &= \text{Atmospheric density} \\ V &= \sqrt{\dot{x}^2 + \dot{y}^2 + \dot{z}^2} \quad .\end{aligned}$$

The density  $\rho$  is a rapidly varying function of altitude, and in addition is a complex function of environmental factors. Furthermore,  $\beta$  is not a constant, but a function of altitude, mach number, and unknown re-entry vehicle parameters. In order to accurately track the vehicle and to predict its future position, it is necessary to determine these parameters as well as the position and velocity. This may be done by estimating the value of  $\beta$ , as well as the other state variables.

In the previous final report on this contract<sup>1</sup>  $\rho$  was assumed to be a known exponential function of altitude, and  $\beta$  was assumed to be of the form

$$\beta = \beta_0 + \beta_1 z$$

where  $\beta_0$  and  $\beta_1$  were continuously estimated as additional state variables. Performance of the estimator so derived is highly dependent on variations of the actual density from its assumed exponential form. Additionally, the assumed model for  $\beta$  is highly inaccurate in certain ranges of altitude, and accurate estimation of  $\beta_0$  and  $\beta_1$  is difficult.

These problems are greatly alleviated and filter performance significantly improved in the present study. The quantity  $\rho/\beta$  is taken as an additional state variable and  $\rho$  is assumed to be only locally exponential—i.e., it is assumed only that  $\rho$  has an altitude gradient

$$\frac{\partial \rho}{\partial z} = -K\rho \quad (20)$$

where  $K$  is a specified constant over each of several ranges of altitude ( $z$ ). The differential equation for the additional state variable  $\rho/\beta$  is then given by

$$(\rho/\beta) \dot{z} = -K(\rho/\beta)z \quad (21)$$

Thus the state vector  $\underline{x}$  has seven components:

$$\begin{aligned} x_1 &= x & x_4 &= \dot{x} \\ x_2 &= y & x_5 &= \dot{y} & x_7 &= \rho/\beta \\ x_3 &= z & x_6 &= \dot{z} \end{aligned} \quad (22)$$

The nonlinear system equations are then rewritten as

$$\dot{\underline{x}} = \underline{f}(\underline{x}) = \begin{bmatrix} x_4 \\ x_5 \\ x_6 \\ -\frac{1}{2}gx_4x_7\sqrt{x_4^2 + x_5^2 + x_6^2} \\ -\frac{1}{2}gx_5x_7\sqrt{x_4^2 + x_5^2 + x_6^2} \\ -\frac{1}{2}gx_6x_7\sqrt{x_4^2 + x_5^2 + x_6^2} - g \\ -Kx_7x_6 \end{bmatrix} \quad (23)$$

These equations are inexact because  $\rho$  and  $\beta$  do not exactly satisfy the assumptions made above, and also because the re-entry vehicle has additional degrees of freedom which are not considered here.<sup>2</sup> To account for these inaccuracies, a vector of random forcing functions  $\underline{w}$ , assumed to be a white Gaussian noise process, is introduced, yielding

$$\dot{\underline{x}}(t) = \underline{f}[\underline{x}(t)] + G\underline{w}(t) \quad (24)$$

where  $G$  is the 7-dimensional identity matrix.

The extended Kalman filter equations of Sec. III are applied by setting

$$\Gamma = G\Delta t$$

$$F(\underline{x}) = \begin{bmatrix} \frac{\partial f_1}{\partial x_j} \end{bmatrix} = \begin{bmatrix} 0 & 0 & 0 & 1 & 0 & 0 & 0 \\ 0 & 0 & 0 & 0 & 1 & 0 & 0 \\ 0 & 0 & 0 & 0 & 0 & 1 & 0 \\ 0 & 0 & 0 & F_{44} & F_{45} & F_{46} & F_{47} \\ 0 & 0 & 0 & F_{54} & F_{55} & F_{56} & F_{57} \\ 0 & 0 & 0 & F_{64} & F_{65} & F_{66} & F_{67} \\ 0 & 0 & 0 & 0 & 0 & F_{76} & F_{77} \end{bmatrix} \quad (25)$$

where

$$F_{44} = -\frac{1}{2}g x_7 \left( \frac{V^2 + x_4^2}{V} \right)$$

$$F_{45} = \frac{-\frac{1}{2}g x_7 x_4 x_5}{V}$$

$$F_{46} = \frac{-\frac{1}{2}g x_7 x_4 x_6}{V}$$

$$F_{47} = -\frac{1}{2} g x_4 V$$

$$F_{54} = F_{45}$$

$$F_{55} = -\frac{1}{2} g x_7 \left( \frac{V^2 + x_5^2}{V} \right)$$

$$F_{56} = \frac{-\frac{1}{2} g x_7 x_5 x_6}{V}$$

$$F_{57} = -\frac{1}{2} g x_5 V$$

$$F_{64} = F_{46}$$

$$F_{65} = F_{56}$$

$$F_{66} = -\frac{1}{2} g x_7 \left( \frac{V^2 + x_6^2}{V} \right)$$

$$F_{67} = -\frac{1}{2} g x_6 V$$

$$F_{76} = -K x_7$$

$$F_{77} = -K x_6 \tag{26}$$

and

$$V = \sqrt{x_4^2 + x_5^2 + x_6^2}$$

## B. Observation Equations

Observations of the target vehicle position are made every  $\Delta t$  seconds by means of a phased-array radar. Measurements are made of the angles  $\alpha$ ,  $\gamma$ , and the range  $r$  in the radar coordinate system of Fig. 1.

The ground coordinates  $x, y, z$  are related to the radar face coordinates by two rotations, representing a tilt of the radar from the vertical and a rotation of the radar from north ( $y$ ), as in Fig. 2. Thus,

$$\begin{bmatrix} x \\ y \\ z \end{bmatrix} = M_1 \begin{bmatrix} x_r \\ y_r \\ z_r \end{bmatrix} \quad (27)$$

where

$$M_1 = \begin{bmatrix} \cos \xi & \sin \tau \sin \xi & \cos \tau \sin \xi \\ -\sin \xi & \sin \tau \cos \xi & \cos \tau \cos \xi \\ 0 & -\cos \tau & \sin \tau \end{bmatrix} \quad (28)$$

$$x_r = r \sin \alpha$$

$$y_r = r \sin \gamma$$

$$z_r = r[1 - \sin^2 \alpha - \sin^2 \gamma]^{\frac{1}{2}} \quad (29)$$

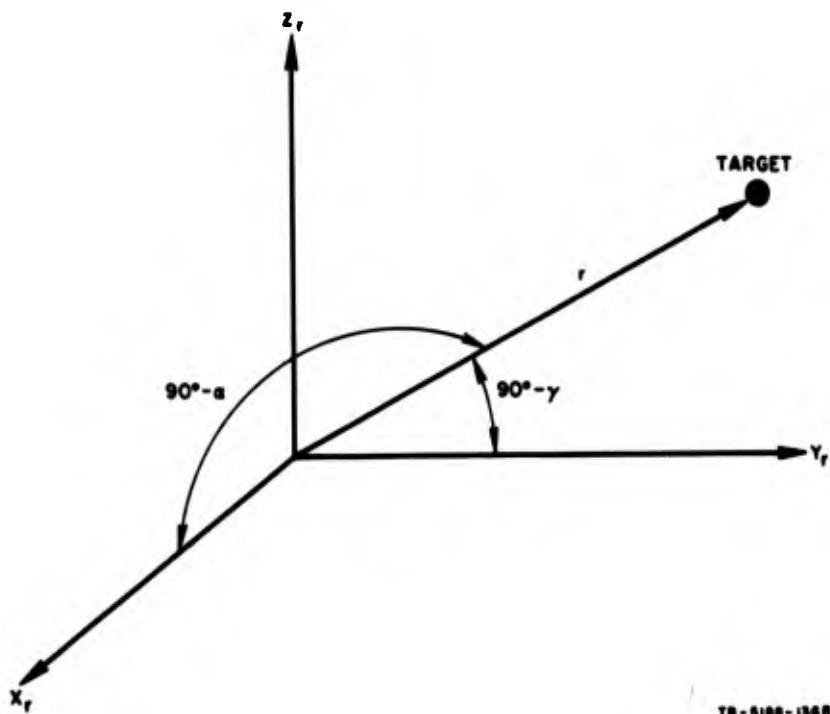
The radar noise is assumed to be a zero mean white Gaussian process with covariance  $R_r(k)$ . This covariance matrix is a function of the particular radar noise model used.

Applying the linearization described in Sec. II-B, the observation equation becomes

$$\underline{z}(k) = H\underline{x}(k) + \underline{v}(k) \quad (30)$$

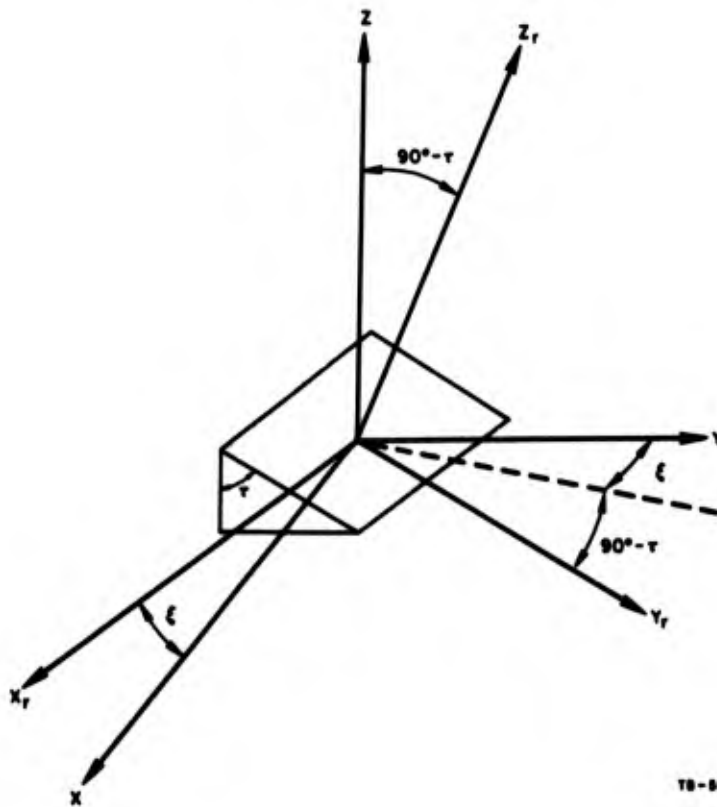
where

$$H = \begin{bmatrix} 1 & 0 & 0 & 0 & 0 & 0 & 0 \\ 0 & 1 & 0 & 0 & 0 & 0 & 0 \\ 0 & 0 & 1 & 0 & 0 & 0 & 0 \end{bmatrix} \quad (31)$$



TB-5188-136R

FIG. 1 RADAR FACE COORDINATES



TB-5188-137R

FIG. 2 RELATION OF RADAR FACE COORDINATES TO GROUND COORDINATES

The covariance of  $\underline{v}$  is

$$R(k) = T(\underline{x})R_r(k)T^T(\underline{x}) \quad (32)$$

where  $T(\underline{x})$ , defined in Eq. (9), has components  $T_{ij}$ , which are most conveniently written in terms of the cartesian radar coordinates  $x_r$ ,  $y_r$ ,  $z_r$ :

$$\begin{aligned} T_{11} &= \frac{x_r}{r} \cos \xi + \frac{y_r}{r} \sin \tau \sin \xi + \frac{z_r}{r} \cos \tau \sin \xi \\ T_{12} &= (z_r^2 + y_r^2)^{1/2} \cos \xi - \frac{x_r}{z_r} (y_r^2 + z_r^2)^{1/2} \cos \tau \sin \xi \\ T_{13} &= (x_r^2 + z_r^2)^{1/2} \sin \tau \sin \xi - \frac{y_r}{z_r} (x_r^2 + z_r^2)^{1/2} \cos \tau \sin \xi \\ T_{21} &= -\frac{x_r}{r} \sin \xi + \frac{y_r}{r} \sin \tau \cos \xi + \frac{z_r}{r} \cos \tau \cos \xi \\ T_{22} &= -(z_r^2 + y_r^2)^{1/2} \sin \xi - \frac{x_r}{r} (y_r^2 + z_r^2)^{1/2} \cos \tau \cos \xi \\ T_{23} &= (x_r^2 + z_r^2)^{1/2} \cos \xi \sin \tau - \frac{y_r}{z_r} (x_r^2 + z_r^2)^{1/2} \cos \tau \cos \xi \\ T_{31} &= -\frac{y_r}{r} \cos \tau + \frac{z_r}{r} \sin \tau \\ T_{32} &= -\frac{x_r}{z_r} (y_r^2 + z_r^2)^{1/2} \sin \tau \\ T_{33} &= -(x_r^2 + z_r^2)^{1/2} \cos \tau - \frac{y_r}{z_r} (x_r^2 + z_r^2)^{1/2} \sin \tau \end{aligned} \quad (33)$$

and

$$r = (x_r^2 + y_r^2 + z_r^2)^{1/2} .$$

The values of  $x_r$ ,  $y_r$ ,  $z_r$  are estimates determined at each sampling instant  $k$  from the predicted state estimate  $\hat{\underline{x}}(k/k - 1)$  by the linear transformation

$$\begin{bmatrix} x_r \\ y_r \\ z_r \end{bmatrix} = M_1^{-1} \begin{bmatrix} \hat{x}_1(k/k - 1) \\ \hat{x}_2(k/k - 1) \\ \hat{x}_3(k/k - 1) \end{bmatrix} \quad (34)$$

All quantities used in implementation of the extended Kalman filter are now specified with the exception of the initial estimate  $\hat{\underline{x}}(0/-1)$ , its error covariance  $S(0/-1)$ , and the covariances  $R_r(k)$  and  $Q(k)$ . The initial estimate is taken to be a program input, and the initial error covariance is chosen to reflect the uncertainty in this estimate. The covariance  $R_r(k)$  is specified by the characteristics of the particular radar system used. The covariance  $Q(k)$ , which is a function of estimated state parameters, is determined so as to compensate for inaccuracies in the system equations.

#### IV NUMERICAL RESULTS FOR THE EXTENDED KALMAN FILTER

Data from four representative trajectories generated by simulation using an accurate model of re-entry dynamics<sup>2</sup> was used to evaluate the performance of the extended Kalman filter described in Sec. III. Re-entry angle for these trajectories is  $21.8^\circ$ . The four cases are the combinations of high or low  $\beta$  and impact at the radar or at a point offset by  $x = 80,000$  ft,  $y = 30,000$  ft from it. For the offset cases, 2 and 4, tracking begins at 150,000 ft; for cases 1 and 3, at 200,000 ft. The trajectories are depicted in Fig. 3. The three position coordinates are corrupted with additive noise representative of actual radar noise.<sup>3,9</sup> The filter operates on these simulated measurements, generating sequential estimates of the seven components of the state vector.

In order to start the computational procedure, an initial state estimate with its error covariance must be specified, along with the actual test data. The initial state estimates, generated as in Ref. 2, are given in Table 1. The initial covariance is the  $7 \times 7$  diagonal matrix

$$S(0/-1) = \begin{bmatrix} 10^6 & & & & & & \\ & 10^6 & & & & & \\ & & 10^6 & & & & \\ & & & 10^6 & & & \\ & & & & 10^6 & & \\ & & & & & 10^6 & \\ & & & & & & S_{77}(0/-1) \end{bmatrix} \quad (35)$$

where

$$S_{77}(0/-1) = 12.86 \times 10^{-14} \exp [-7.38 \times 10^{-5} \hat{x}_3(0/-1)] .$$

The magnitude of the initial position error varies, over the four cases, between 10% and 13% of the magnitude of the initial range; the initial

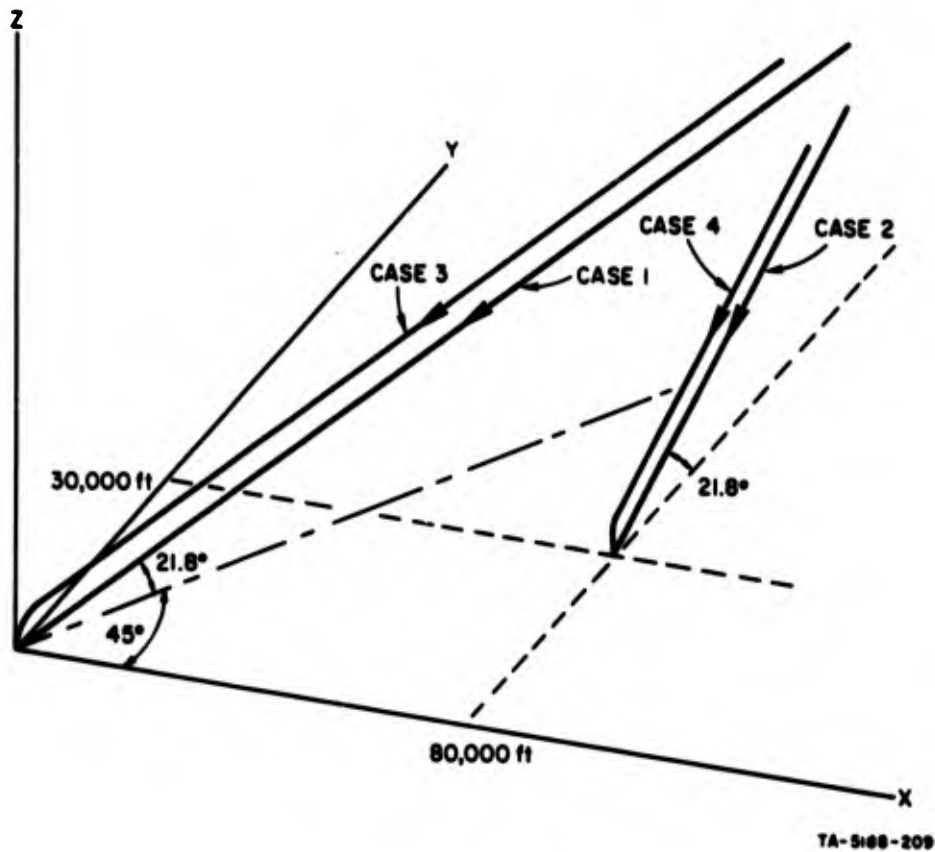


FIG. 3 TEST TRAJECTORIES

Table 1  
INITIAL CONDITIONS

	$x_1$ (ft)	$x_2$ (ft)	$x_3$ (ft)	$x_4$ (ft/sec)	$x_5$ (ft/sec)	$x_6$ (ft/sec)	$x_7$ (sec <sup>2</sup> /ft <sup>2</sup> )
Case 1							
Actual: $\underline{x}(0)$	338110	338110	199910	15297	15297	8653	$5.220 \times 10^{-10}$
Estimate: $\hat{\underline{x}}(0/-1)$	290952	292135	199911	16046	14466	12751	$6.118 \times 10^{-10}$
Error	47158	45975	1	749	831	4098	
Case 2							
Actual: $\underline{x}(0)$	80000	391520	149910	0	21634	8653	$9.719 \times 10^{-10}$
Estimate: $\hat{\underline{x}}(0/-1)$	80111	335179	149608	4065	21277	11848	$2.376 \times 10^{-9}$
Error	111	56341	302	4065	357	3195	
Case 3							
Actual: $\underline{x}(0)$	317000	317000	199100	15297	15297	8653	$2.124 \times 10^{-9}$
Estimate: $\hat{\underline{x}}(0/-1)$	279283	280371	200115	16443	14993	12460	$6.118 \times 10^{-10}$
Error	37717	36623	1015	1146	304	3807	
Case 4							
Actual: $\underline{x}(0)$	80000	360440	149910	0	21633	8653	$5.557 \times 10^{-9}$
Estimate: $\hat{\underline{x}}(0/-1)$	90093	318857	149842	1187	20891	11592	$2.376 \times 10^{-9}$
Error	9093	41583	68	1187	742	2939	

velocity error magnitude varies between 14% and 22.5% of the initial velocity magnitude. The initial error in  $\rho/\beta$  represents an initial error in the value of  $\beta$  of between 15% and 261% of  $\beta$ 's initial value, depending on the case.

The measurement noise covariance,  $R_p(k)$ , is obtained from a model of actual radar noise characteristics based on work by Bell Telephone Laboratories.<sup>3</sup> The expressions for the elements of this covariance are found in Ref. 9.

The covariance  $Q(k)$ , associated with the random forcing function  $\underline{w}$ , compensates for the model inaccuracies described earlier. A good choice was determined experimentally to be the matrix



velocity and acceleration at this point are less than 300 ft/sec and 2g, respectively. The errors in position and velocity decrease to much lower values at later times. In all cases, error in the  $\beta$  estimate is very small, less than 125 lb/ft<sup>2</sup>, after 12 or 13 seconds. It should be noted that acceleration is not computed directly by the filter, but is calculated from the state estimate using Eqs. (19) of Sec. III. The errors in the position estimates, Figs. 5(a), 6(a), 7(a), and 8(a), compare very favorably with the measurement errors, indicating significant filtering. More importantly, however, the filter is able to derive excellent estimates of velocity and  $\rho/\beta$ , which are necessary for predicting the state of the vehicle at a future time. Figures 5(b), 6(b), 7(b), and 8(b) show the errors in these velocity estimates; Figs. 5(c), 6(c), 7(c), and 8(c) show the actual and estimated  $\beta$  for each case, where the estimated  $\beta$  was found from the state estimate  $\hat{x}_7(k/k)$  by assuming  $\hat{\beta}(k/k) = \rho(k)/\hat{x}_7(k/k)$ , where  $\rho$  is the atmospheric density used in the test trajectory simulation. The errors in the acceleration estimates are shown in Figs. 5(d), 6(d), 7(d), and 8(d).

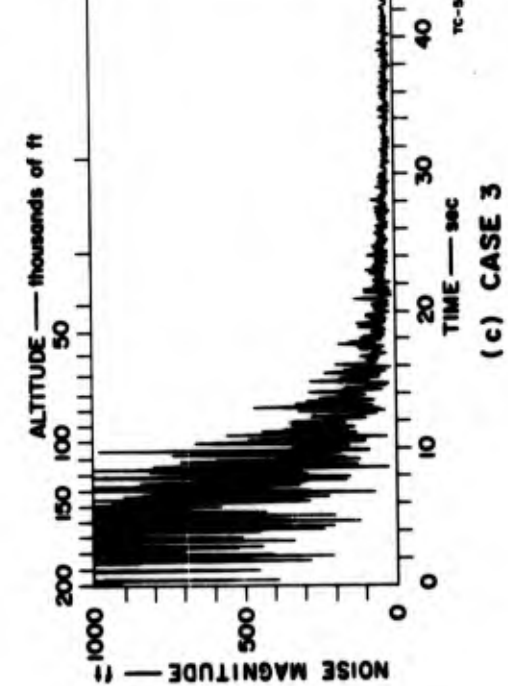
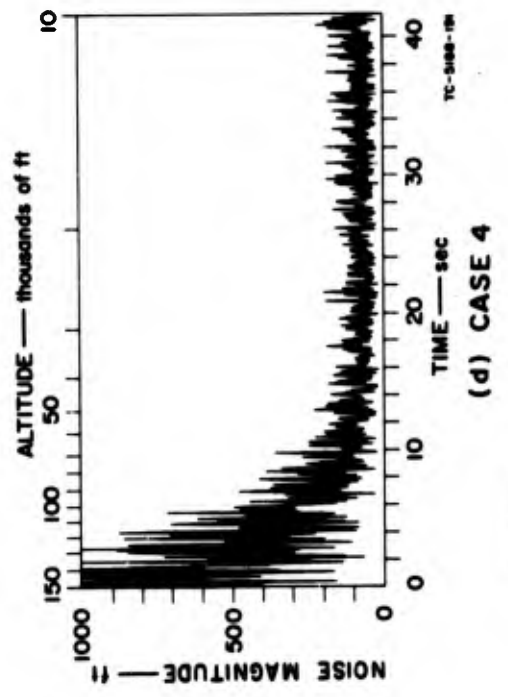
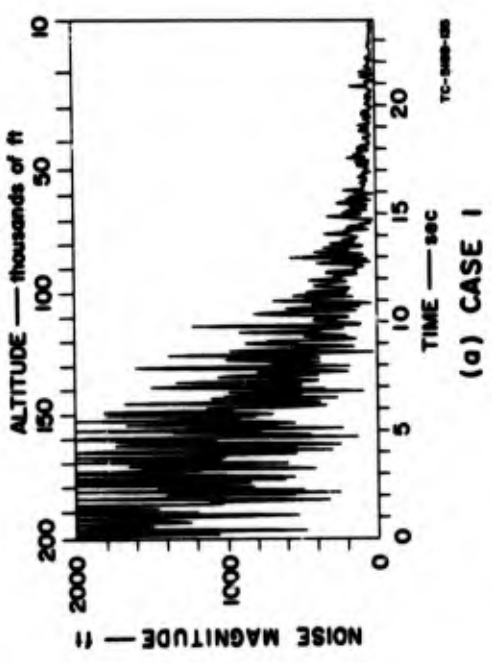
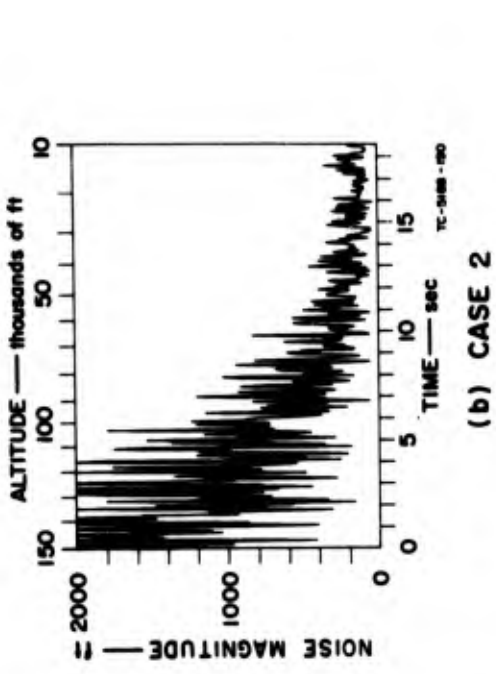
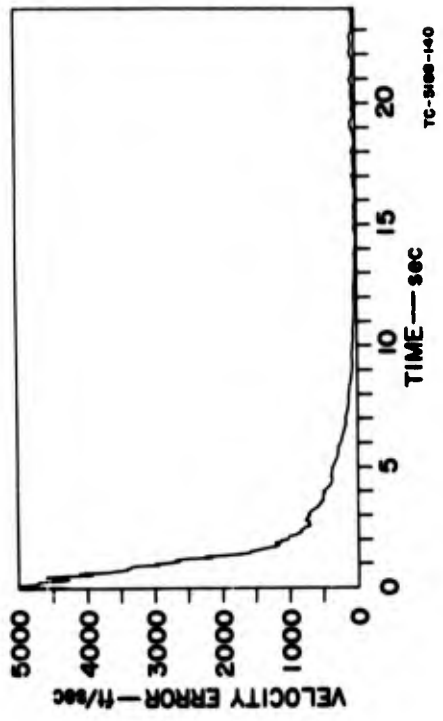
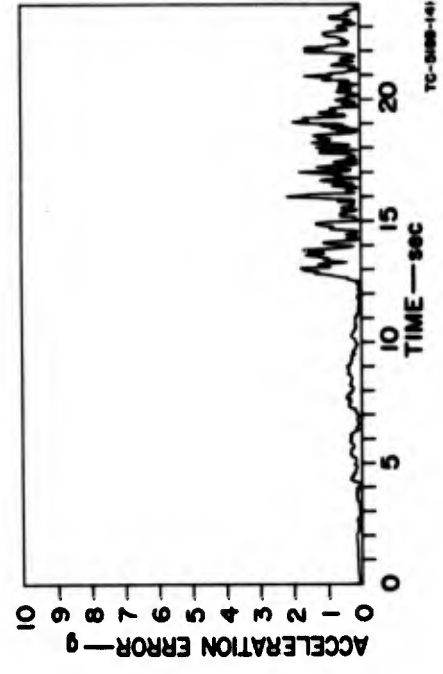


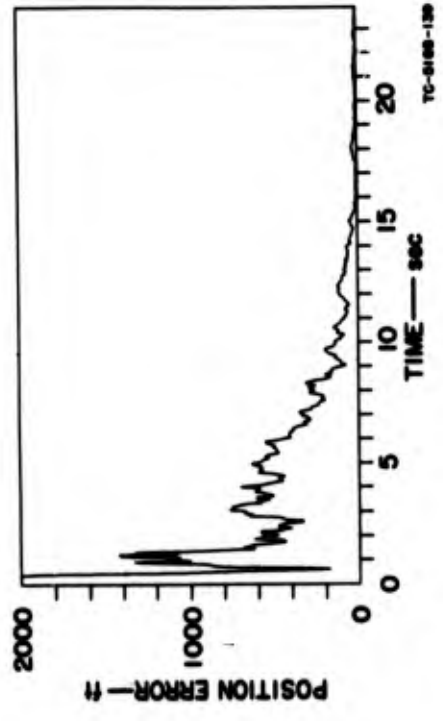
FIG. 4 MEASUREMENT NOISE



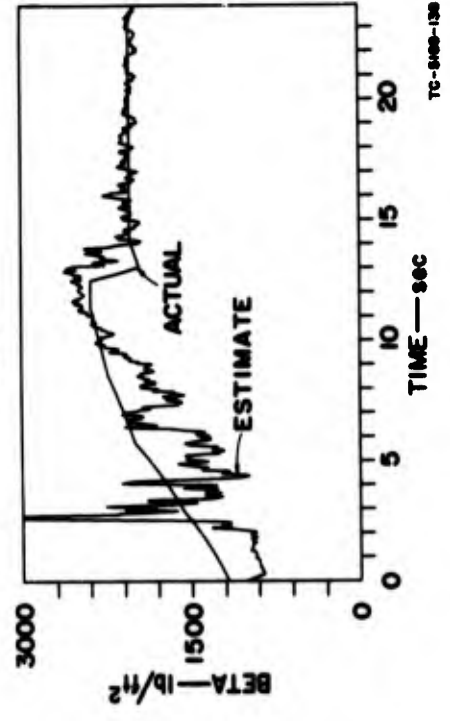
(b)



(d)



(a)



(c)

FIG. 5 EXTENDED KALMAN FILTER -- CASE 1

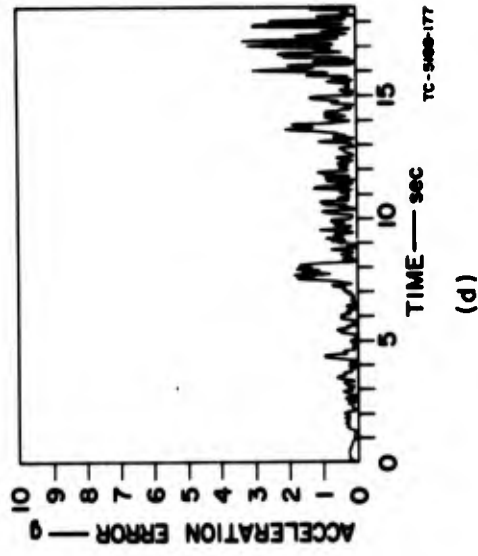
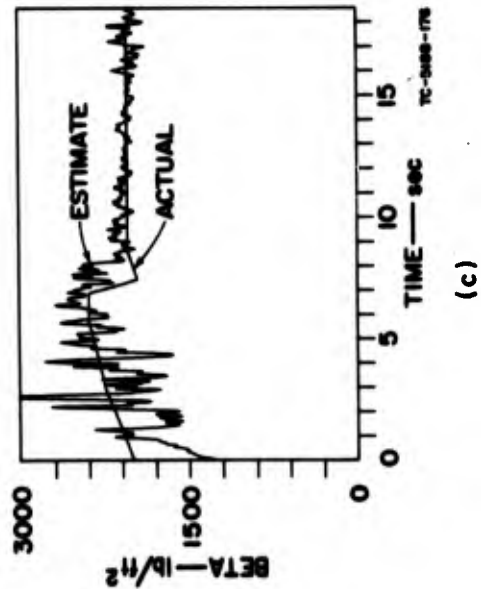
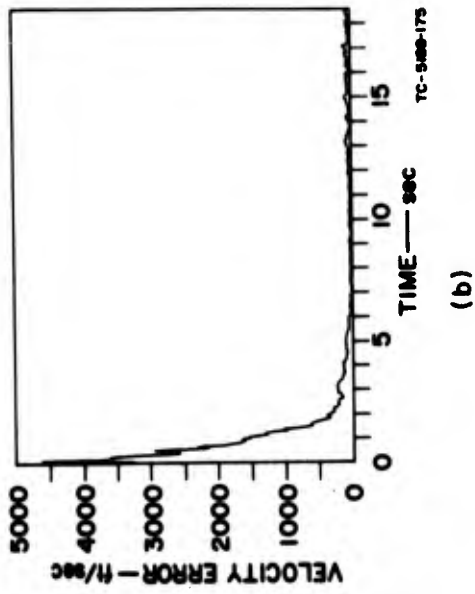
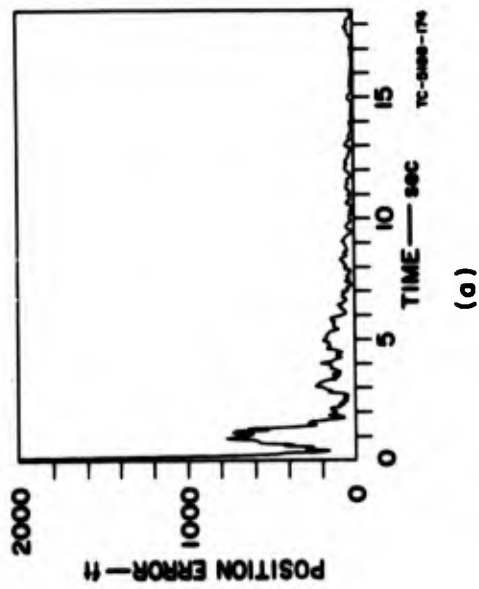


FIG. 6 EXTENDED KALMAN FILTER — CASE 2

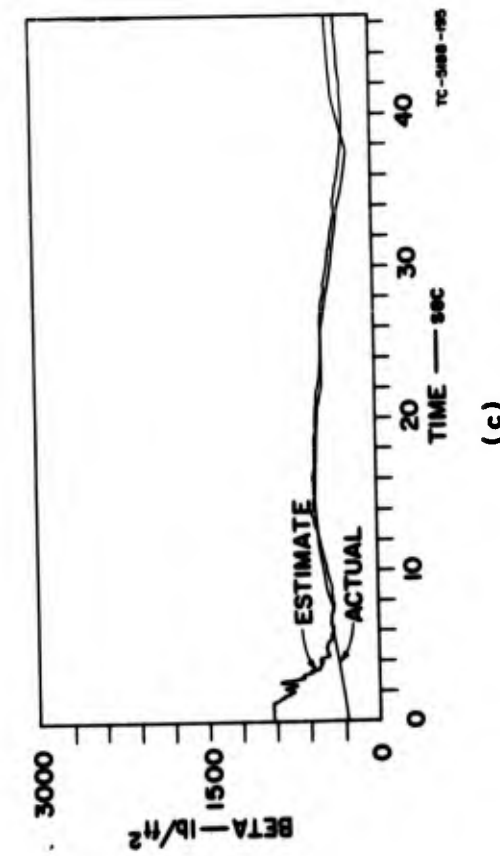
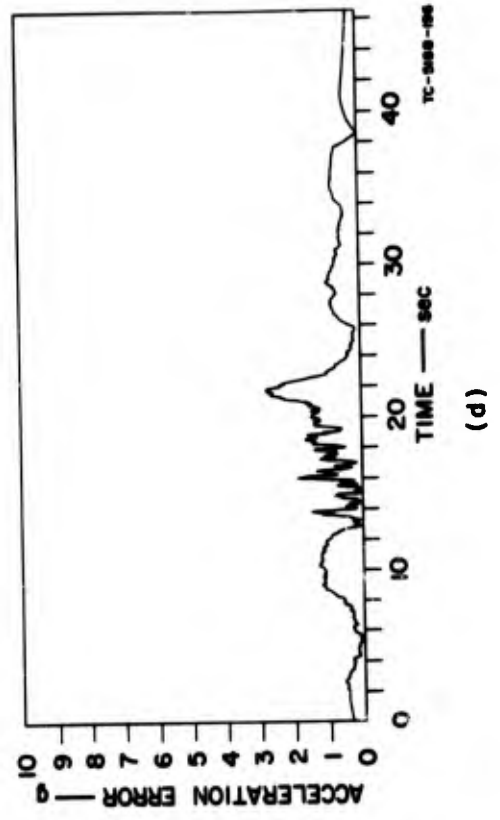
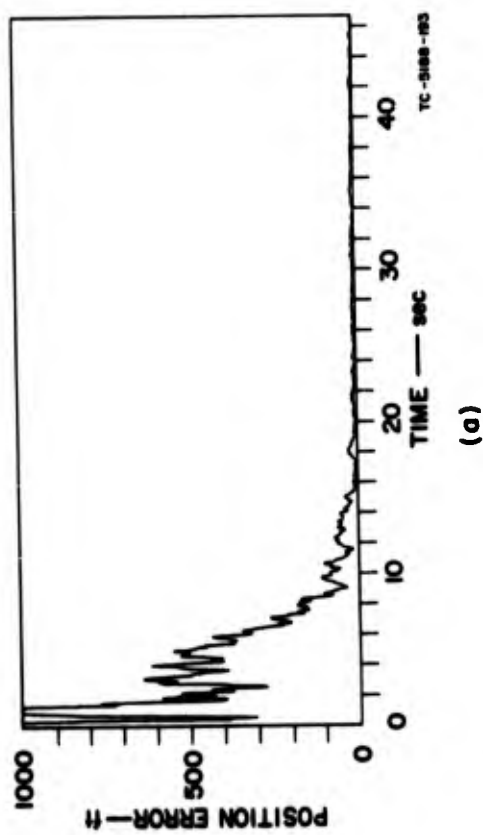
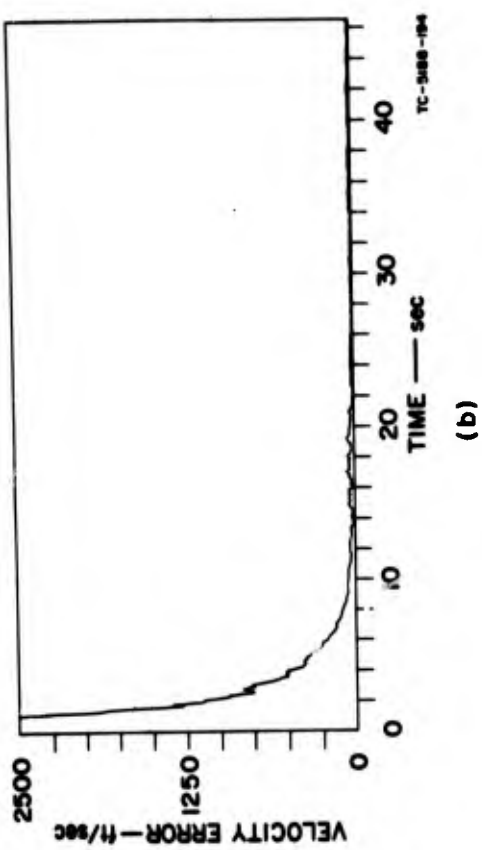
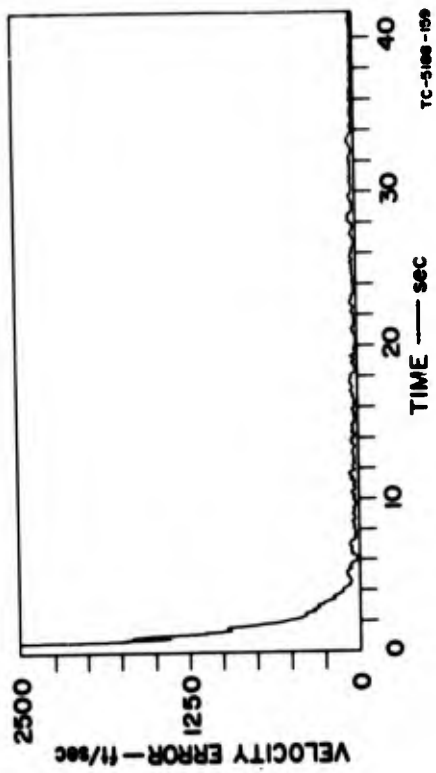
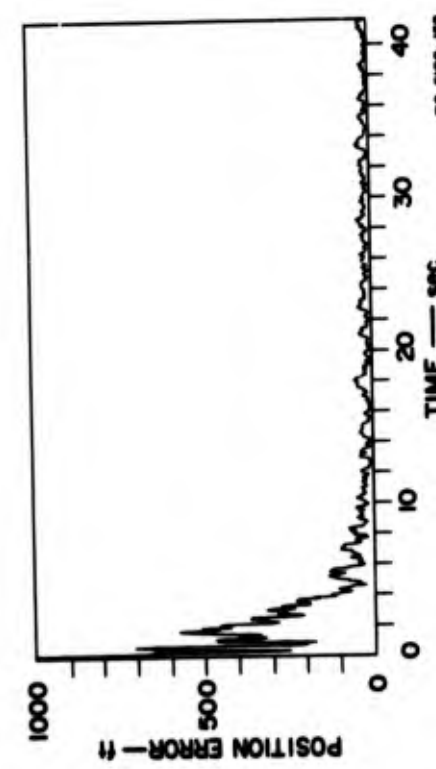


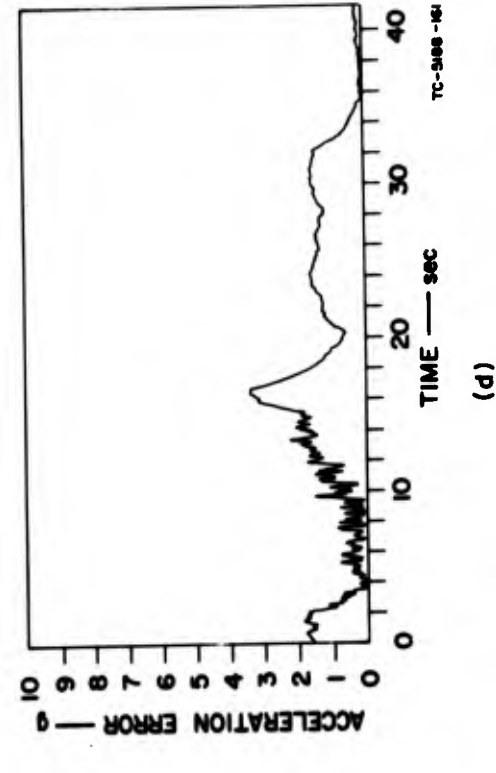
FIG. 7 EXTENDED KALMAN FILTER — CASE 3



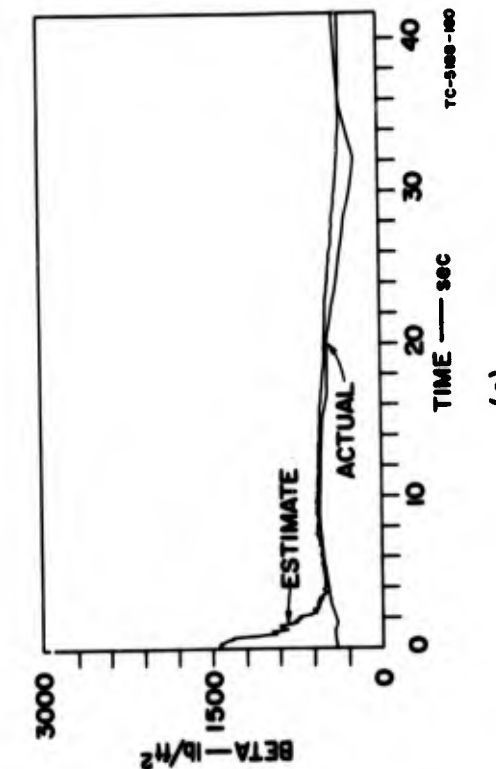
(a)



(b)



(c)



(d)

FIG. 8 EXTENDED KALMAN FILTER — CASE 4

## V COMPARISON WITH POLYNOMIAL FILTERS

### A. Qualitative Comparison

Other types of filters have been proposed for estimating the state of a ballistic missile. In particular, these include polynomial filters; the exponentially weighted polynomial filter is described in Appendix C of Ref. 1, and the finite memory polynomial filter is described in Appendix B of this reference. Since the polynomial filters do not employ all of the *a priori* knowledge (e.g., the equations of motion for the ballistic missile and the known statistics of the radar noise), it is reasonable to expect the performance of the extended Kalman filter to be better than that of the various polynomial filters. However, the extended Kalman filter will require more computation time than the polynomial filters. Further details on these points appear in Ref. 2.

In Ref. 5 it was shown that a second-order polynomial filter (for each coordinate:  $x$ ,  $y$ ,  $z$ ) is equivalent to a Kalman filter based on several assumptions. These assumptions include constant target acceleration in the equations of motion and no correlation between the components of the measurement noise vector. The Kalman filter obtained using the above assumptions differs appreciably from the extended Kalman filter described in Sec. II-B and would be expected to exhibit inferior performance.

### B. Comparison with the Exponentially Weighted Polynomial Filter

In order to obtain quantitative comparisons of performance with the extended Kalman filter, an exponentially weighted polynomial filter was implemented on a digital computer. Using state variable notation, the second-order polynomial filter for the  $x$  coordinate can be described by the following discrete equation (the equations for the  $y$  and  $z$  coordinates are identical):

$$\begin{aligned}
& \begin{bmatrix} \hat{x}(k/k) \\ \hat{\dot{x}}(k/k) \\ \hat{\ddot{x}}(k/k) \end{bmatrix} \\
& = \begin{bmatrix} \alpha^3 & \alpha^3 \Delta t & \frac{\alpha^3 (\Delta t)^2}{2} \\ \frac{-(3\alpha^3 - 3\alpha^2 - 3\alpha + 3)}{2\Delta t} & \frac{-(3\alpha^3 - 3\alpha^2 - 3\alpha + 1)}{2} & \frac{-(3\alpha^3 - 3\alpha^2 - 3\alpha - 1)\Delta t}{4} \\ \frac{(\alpha - 1)^3}{(\Delta t)^2} & \frac{(\alpha - 1)^3}{\Delta t} & \frac{1}{2} (\alpha^3 - 3\alpha^2 + 3\alpha + 1) \end{bmatrix} \begin{bmatrix} \hat{x}(k-1/k-1) \\ \hat{\dot{x}}(k-1/k-1) \\ \hat{\ddot{x}}(k-1/k-1) \end{bmatrix} \\
& + \begin{bmatrix} 1 - \alpha^3 \\ \frac{(3\alpha^3 - 3\alpha^2 - 3\alpha + 3)}{2\Delta t} \\ \frac{1}{(\Delta t)^2} (1 - \alpha)^3 \end{bmatrix} x_m(k)
\end{aligned} \tag{39}$$

where  $x_m$  is the noisy measurement of  $x$ —i.e.,  $x_m$  is equivalent to  $z_1$  of Eq. (30). In this polynomial filter,  $\hat{x}$ ,  $\hat{y}$ , and  $\hat{z}$  are considered to be state variables; the estimate  $\hat{\beta}$  is a derived quantity, which is given by the algebraic expression

$$\hat{\beta}(k/k) = \frac{\rho g [\hat{\dot{x}}^2(k/k) + \hat{\dot{y}}^2(k/k) + \hat{\dot{z}}^2(k/k)]}{2 [\hat{\ddot{x}}(k/k) + \hat{\ddot{y}}^2(k/k) + \hat{\ddot{z}}^2(k/k)]^{1/2}} \tag{40}$$

The time constant  $\tau$  of the polynomial filter is given by

$$\alpha = e^{-\frac{\Delta t}{\tau}} \tag{41}$$

The exponentially weighted polynomial filter was run using the same data for Cases 1, 2, 3, and 4 as the extended Kalman filter. The data (trajectories, measurement noise, and initial conditions) are summarized in Sec. IV. After an extensive tuning process, it was found that the overall performance of the polynomial filter on the four cases was best for  $\alpha = 0.91$ .

In order to compare the performance of the polynomial filter ( $\alpha = 0.91$ ) with that of the extended Kalman filter, the numerical results have been plotted in Figs. 9 through 12, with the same scales as were used for the extended Kalman filter (Figs. 5 through 8).

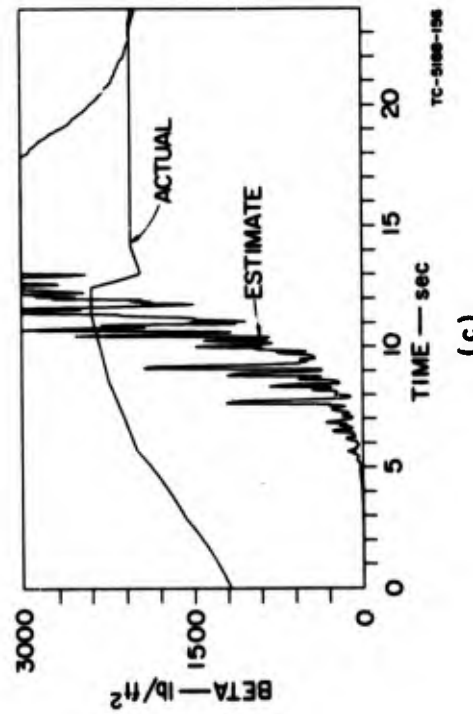
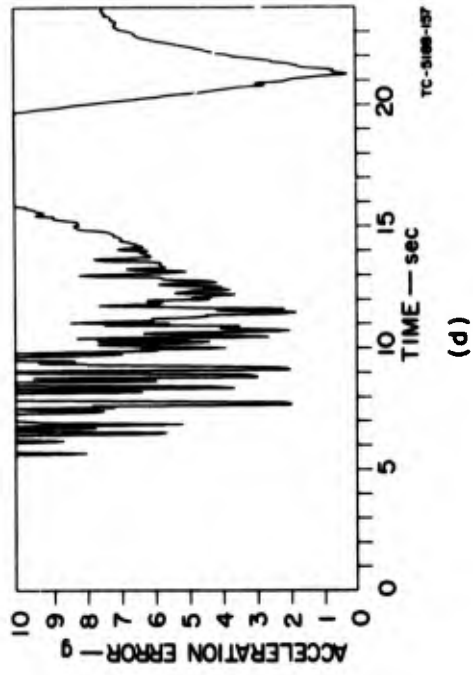
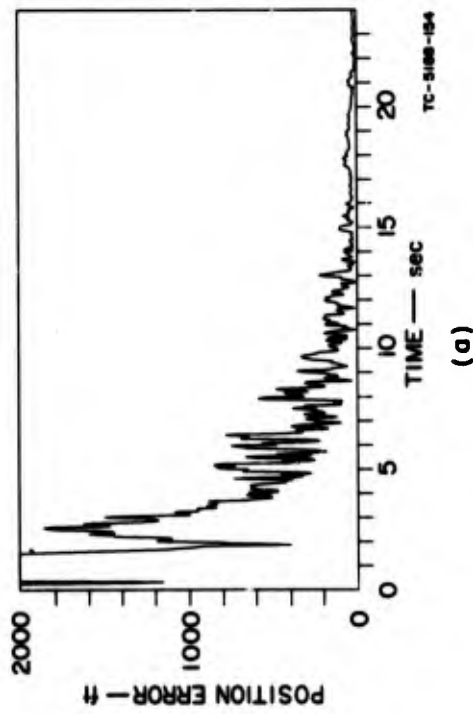
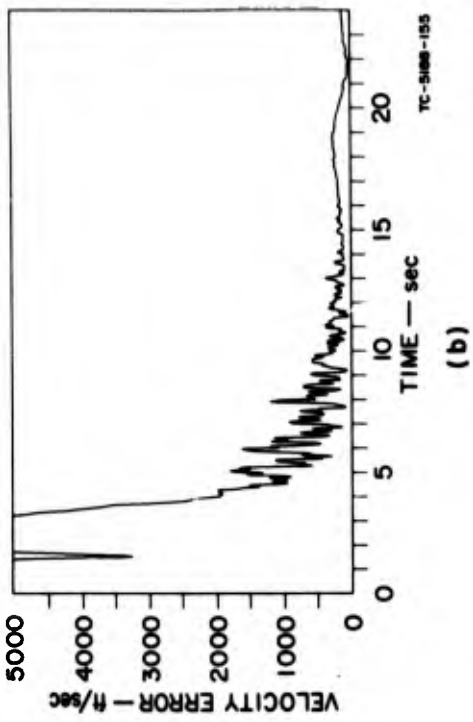
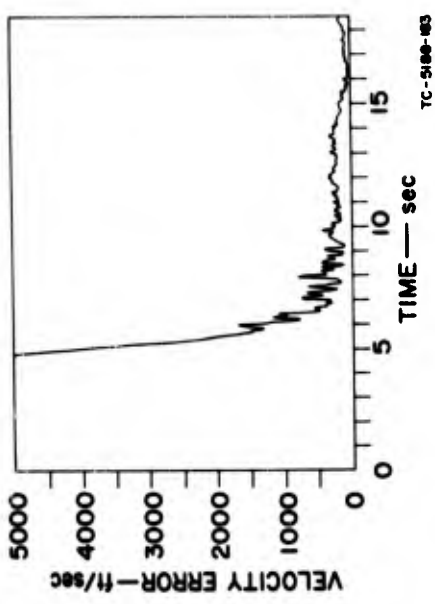
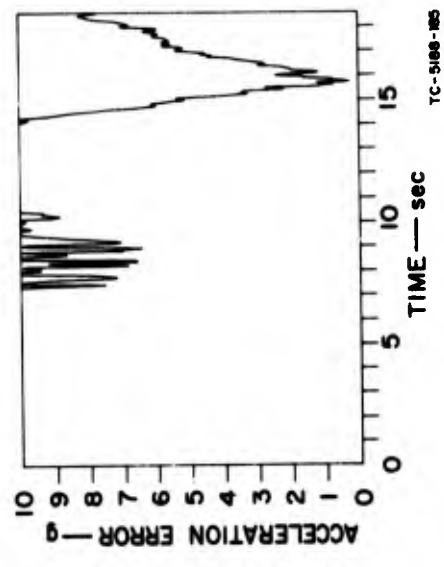


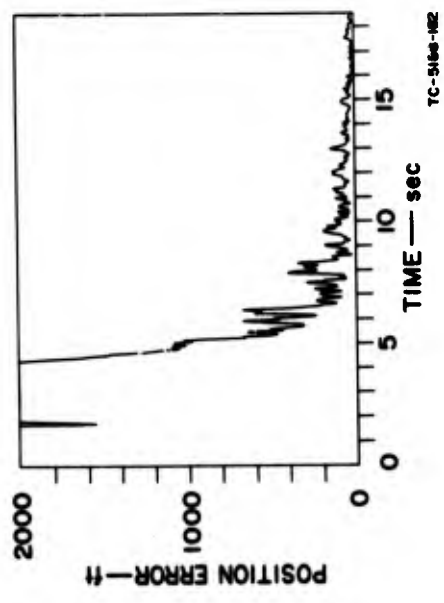
FIG. 9 POLYNOMIAL FILTER — CASE 1



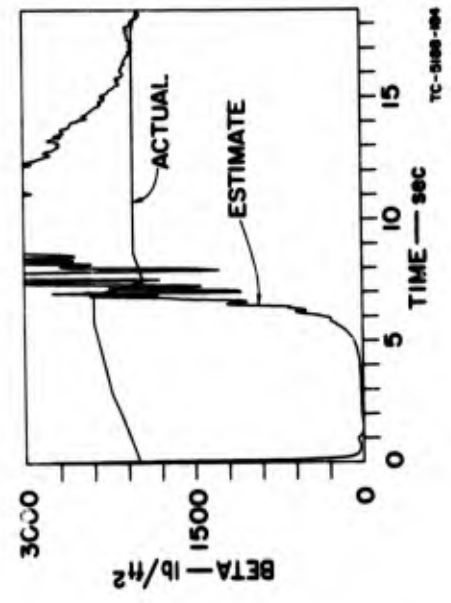
(b)



(d)



(a)



(c)

FIG. 10 POLYNOMIAL FILTER — CASE 2

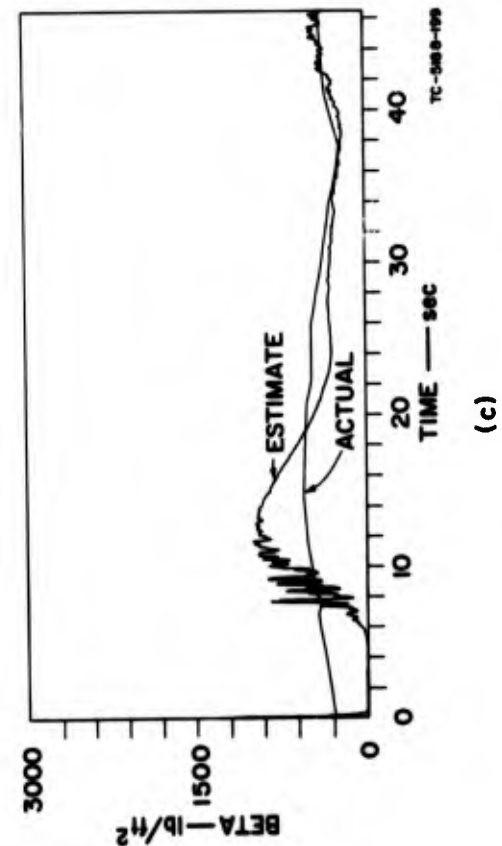
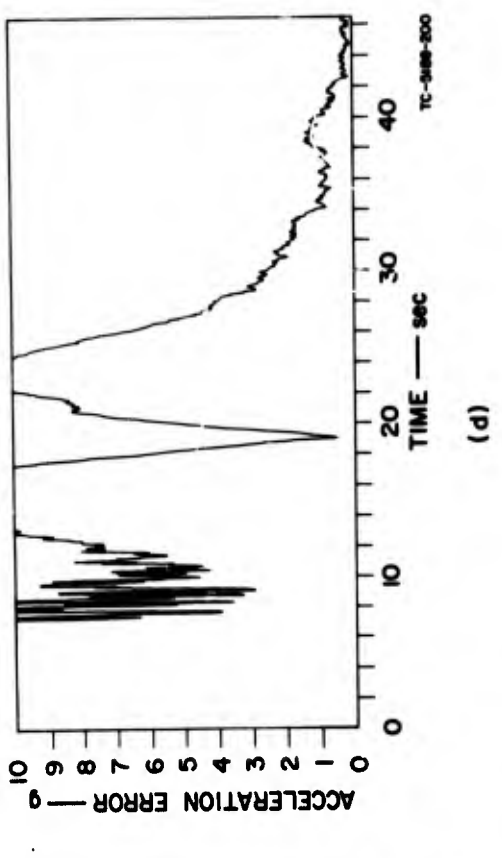
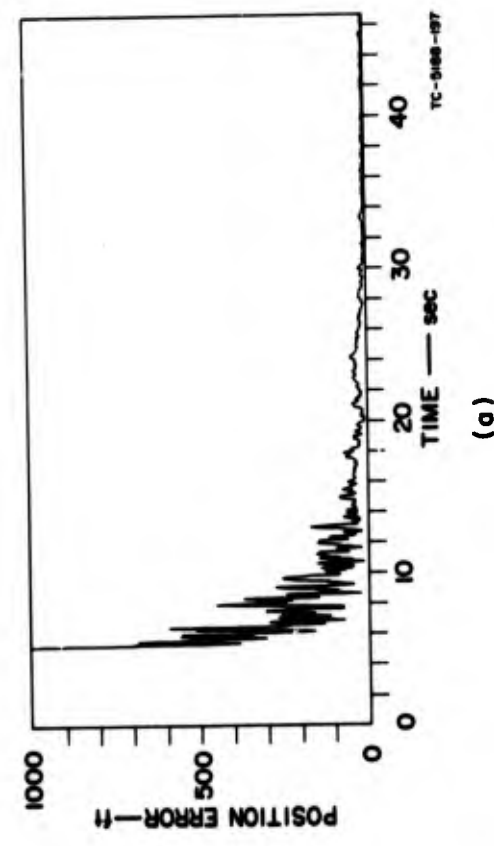
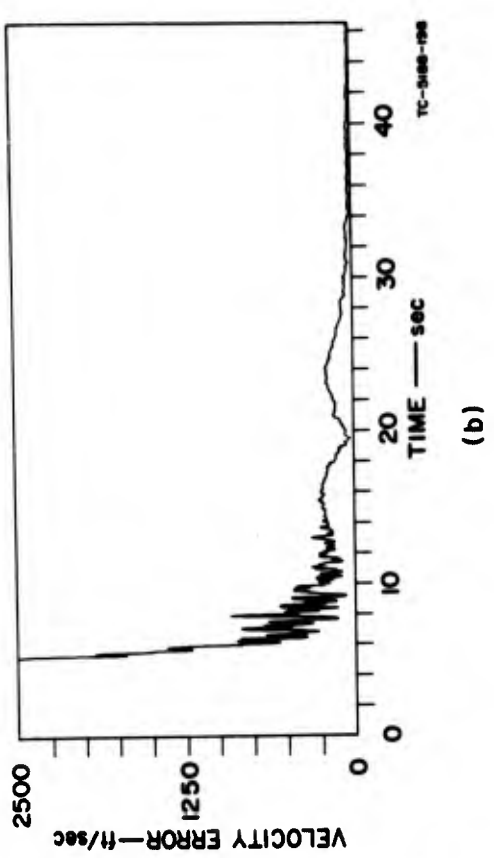
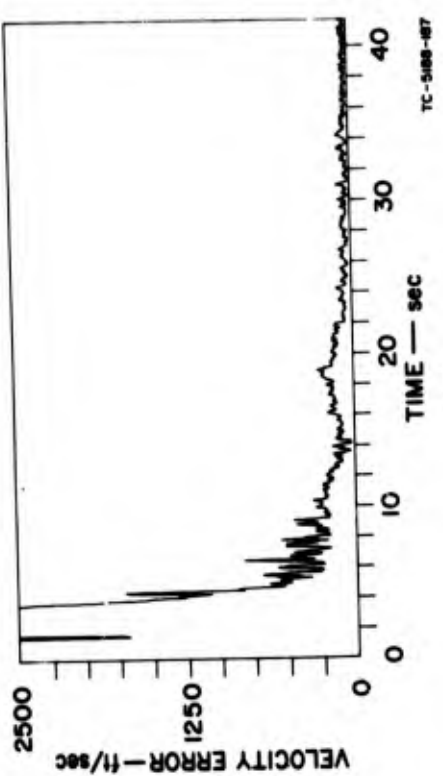
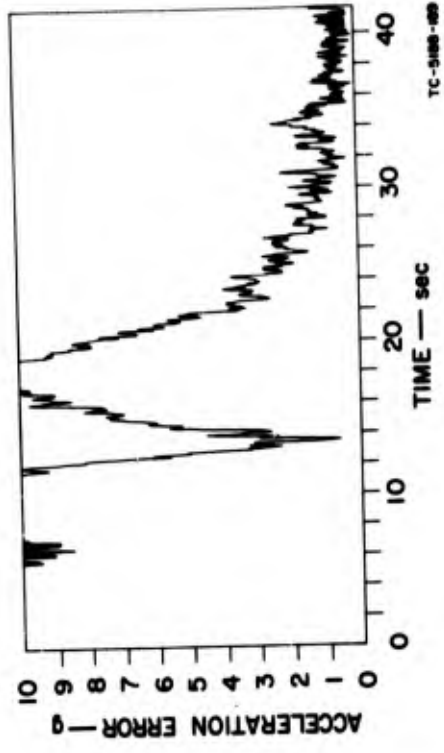


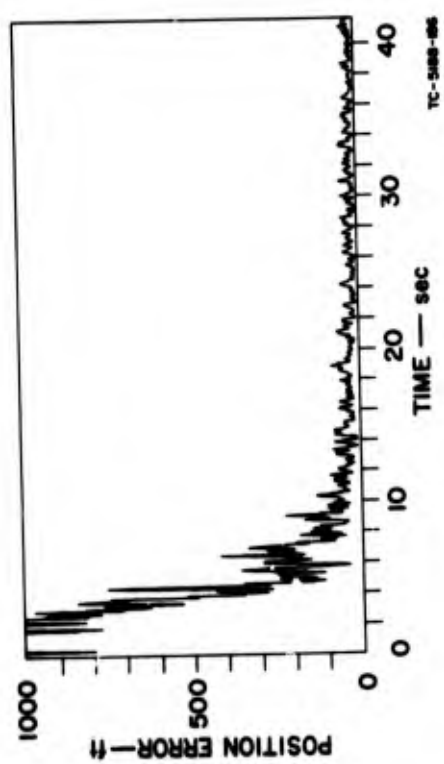
FIG. 11 POLYNOMIAL FILTER — CASE 3



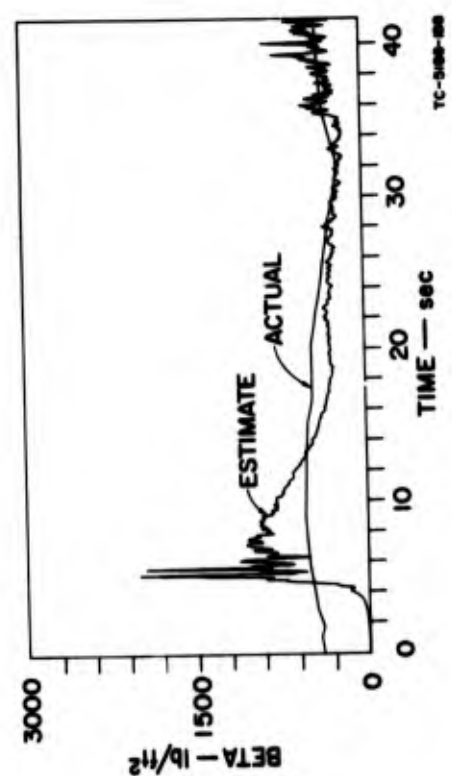
(b)



(d)



(a)



(c)

FIG. 12 POLYNOMIAL FILTER — CASE 4

## VI EFFECTS OF VARIATION IN DATA RATE AND DATA INTERRUPTION

### A. Variation in Data Rate

Because of the direct dependence of computational requirements on the data-sampling rate of the Kalman filter, it is desirable to make this rate as low as possible consistent with good filter performance. The interval between trajectory observations was successively increased from 0.05 sec to 0.10 sec, to 0.25 sec, for Cases 1 and 4 defined in Fig. 3; the results are presented in Figs. 13 through 16. These results show that halving the data rate (0.10-sec intervals) has very little effect on filter accuracy.

Reduction of the data rate by a factor of 5 (0.25-sec intervals) tends to degrade performance somewhat in both Case 1 and Case 4. The errors in the position and velocity estimates after 3.5 sec are increased by factors of about 5 and 3, respectively. Acceleration and  $\beta$  errors are substantially unchanged, except at a few points where they are increased by factors of 2 and 3, respectively.

It should be noted that at this slowest data rate the filter performs more accurately on the relatively slower Case 4 vehicle than on that of Case 1.

### B. Data Interruption

During the radar tracking of a re-entry vehicle, measurements may become unavailable for some interval of time. Such interruption of data may result from blackout, countermeasures, power system transients, and other special operational situations. In these intervals the Kalman filter state estimate is calculated by integrating the equations of motion, with the state estimate at the time when input data is lost as an initial condition. Since there is an estimation error at that time, and since the equations of motion and numerical integration formula used are inexact, the state estimate may be expected to diverge as long as no new data is received. An interruption of data for a one-second duration was introduced at four points in the runs of Cases 1 and 4. The interruptions occurred 4, 8, 12, and 16 seconds after tracking began. The results are presented in Figs. 17 and 18.

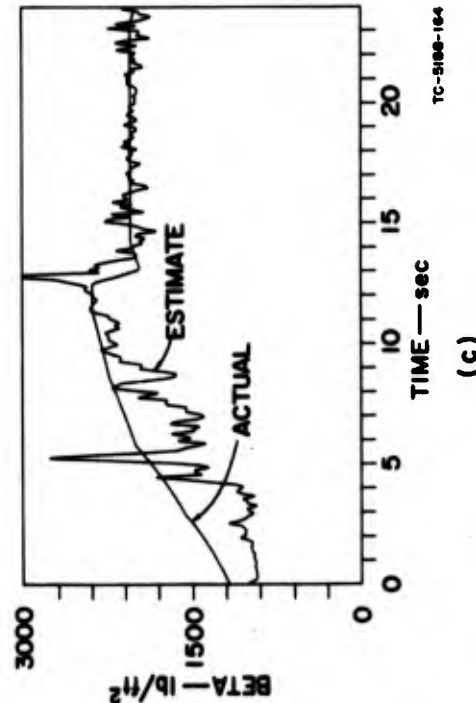
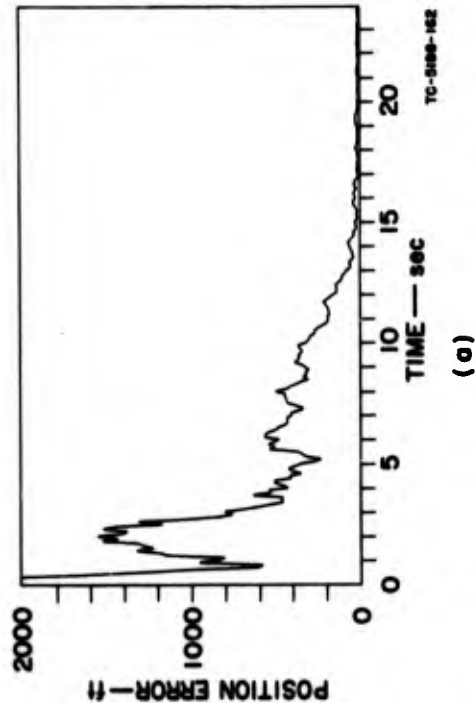
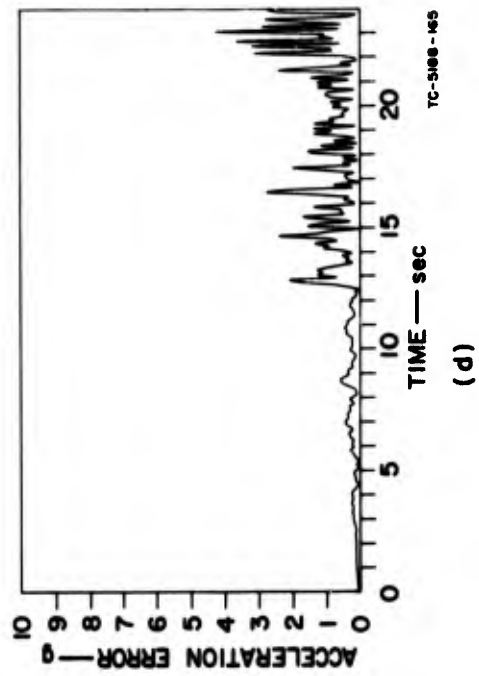
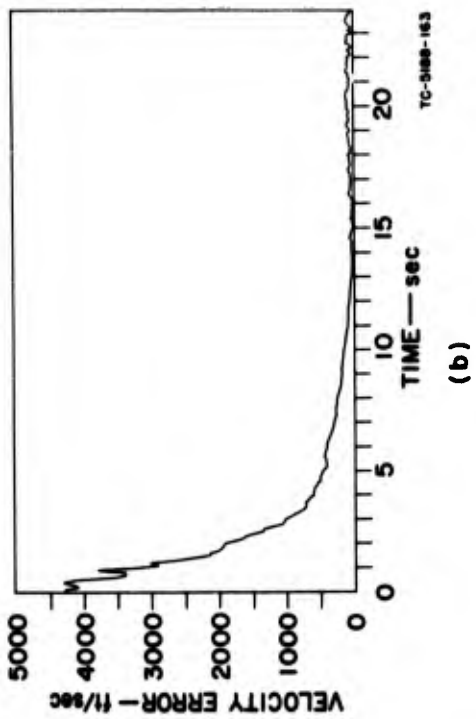


FIG. 13 EXTENDED KALMAN FILTER — CASE 1,  $\Delta t = 0.10$  sec

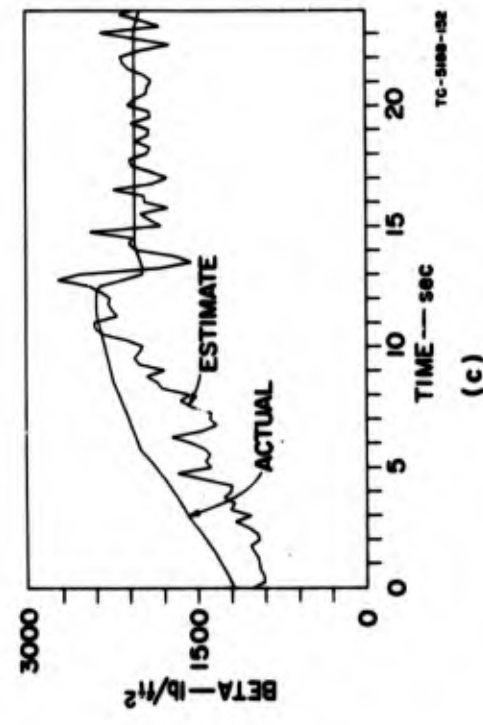
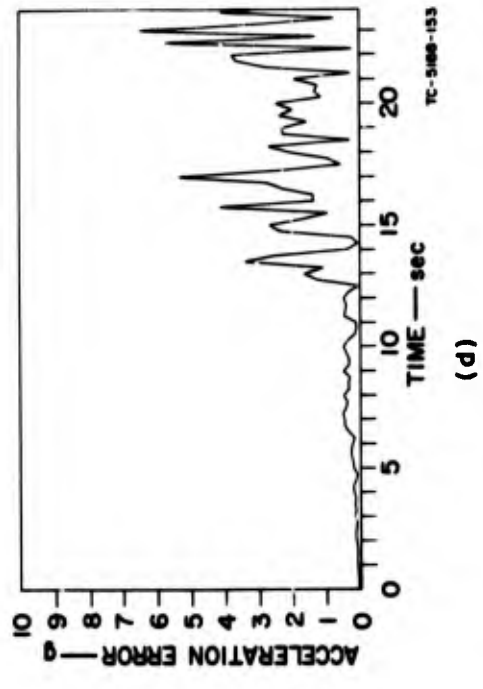
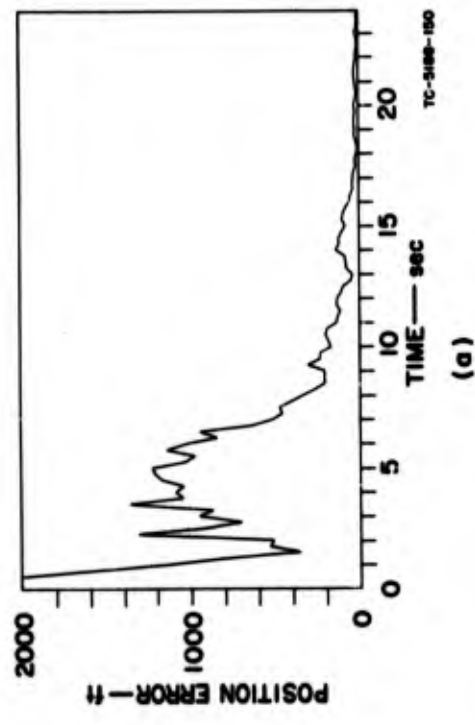
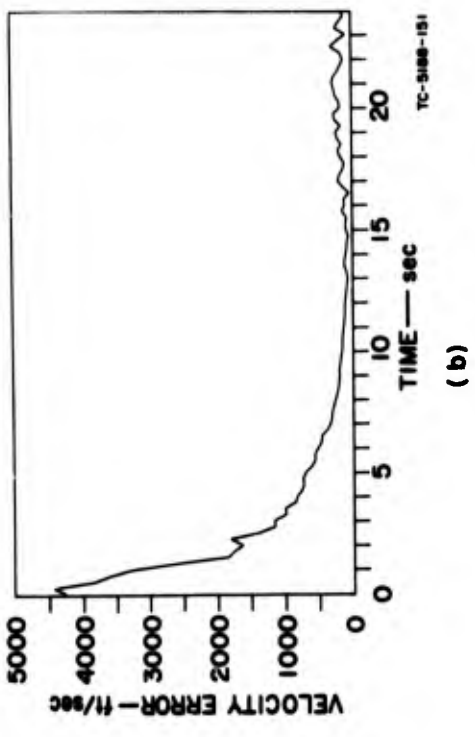


FIG. 14 EXTENDED KALMAN FILTER — CASE 1,  $\Delta t = 0.25$  sec

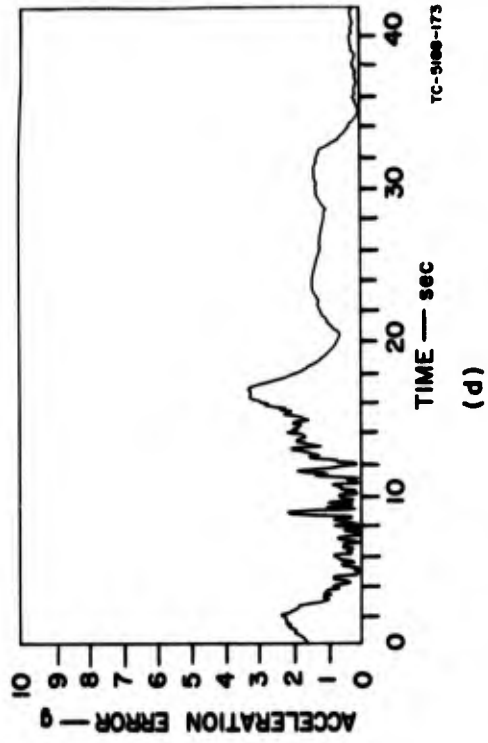
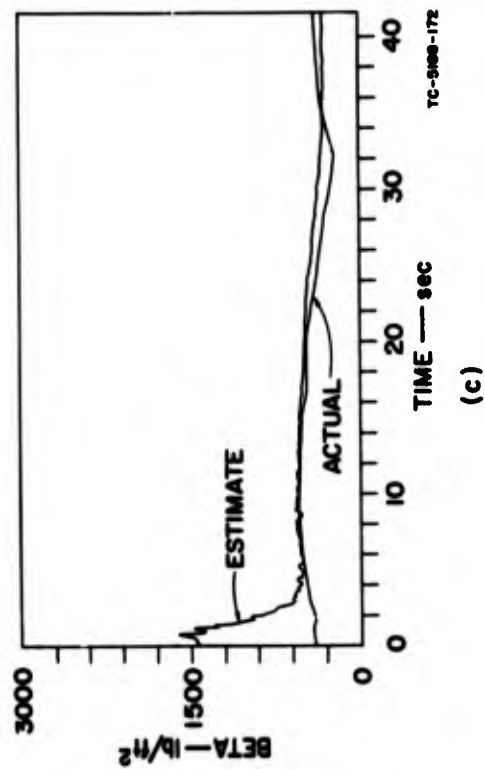
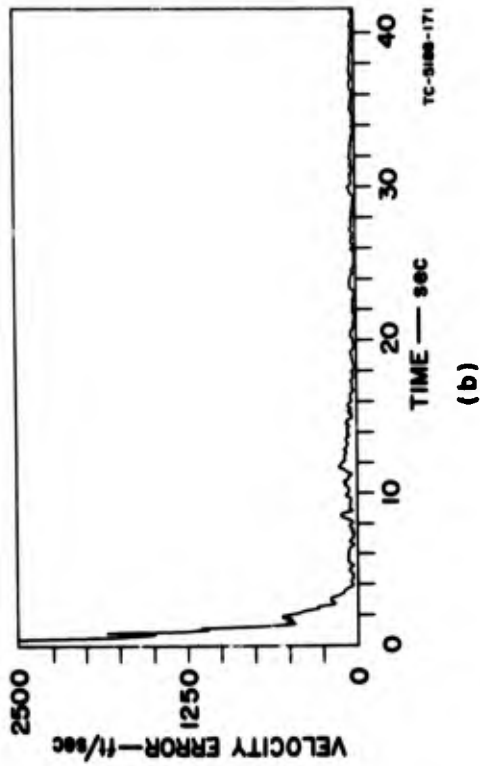
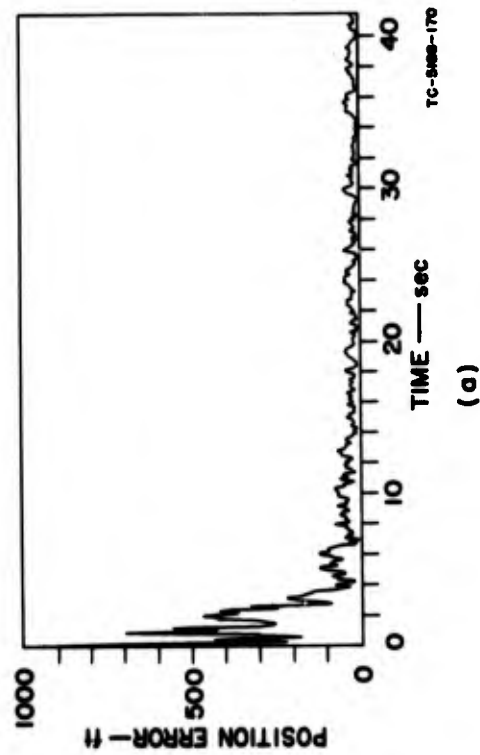


FIG. 15 EXTENDED KALMAN FILTER — CASE 4,  $\Delta t = 0.10$  sec

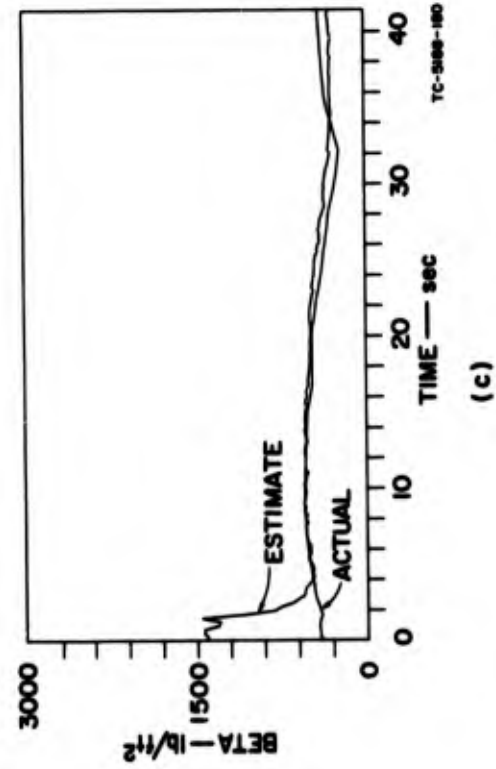
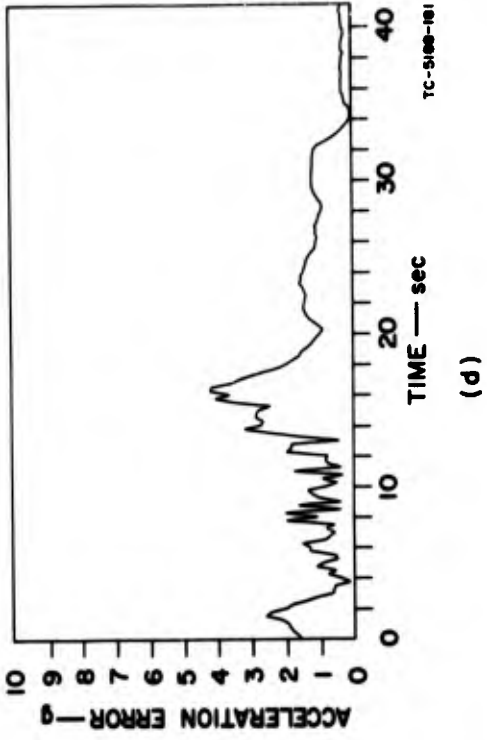
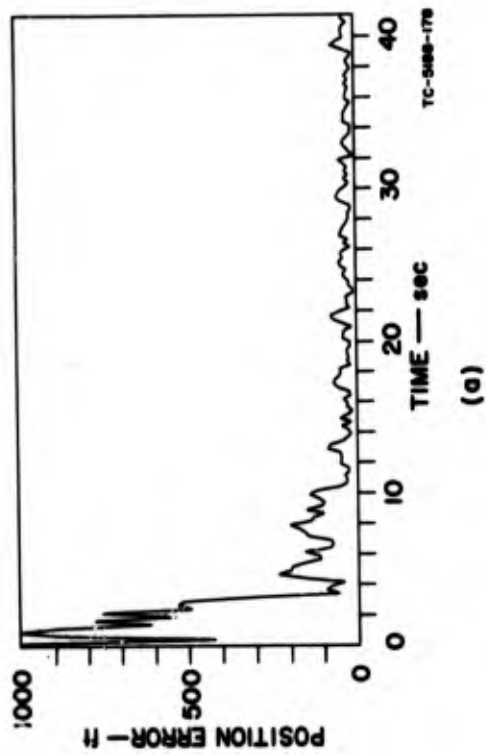
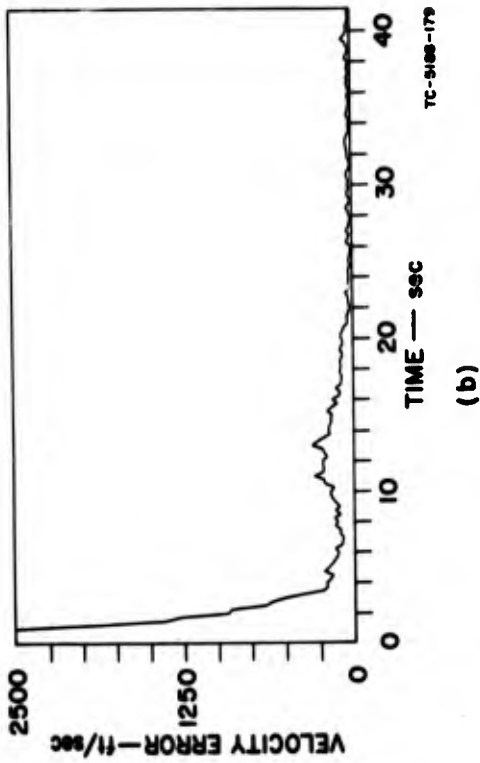
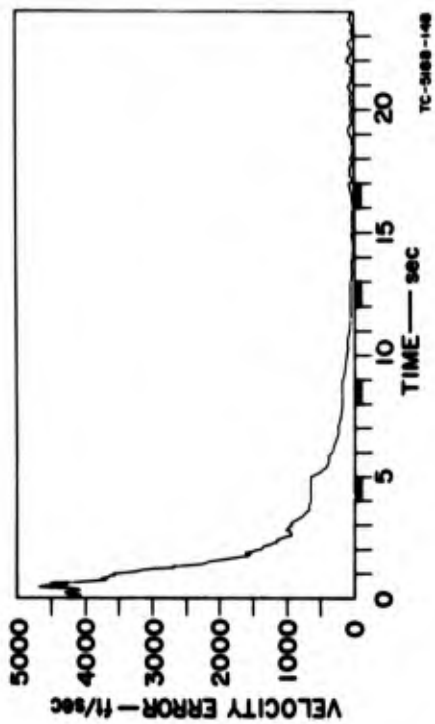
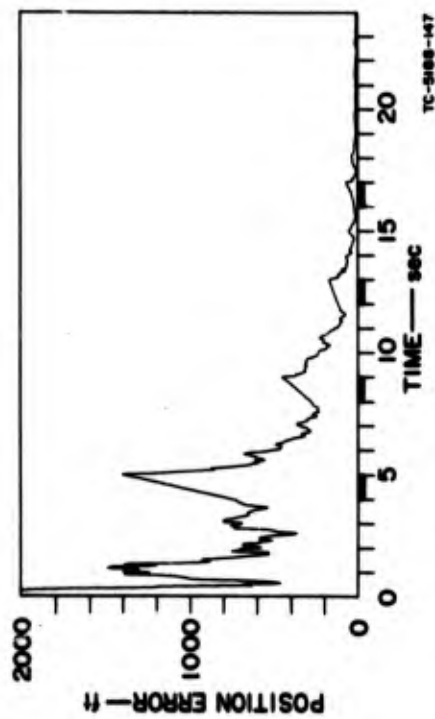


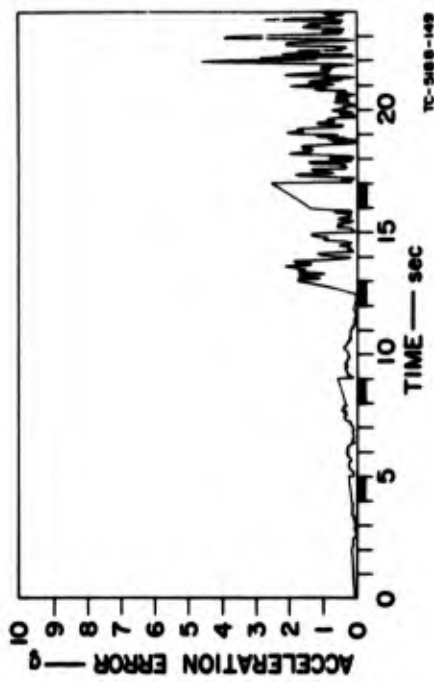
FIG. 16 EXTENDED KALMAN FILTER — CASE 4,  $\Delta t = 0.25$  sec



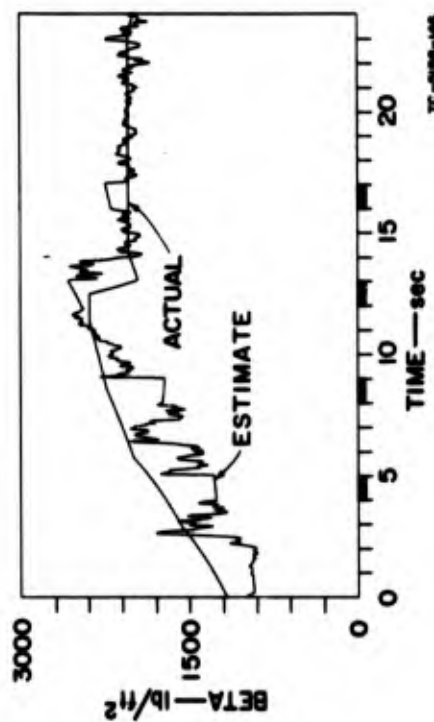
(a)



(b)

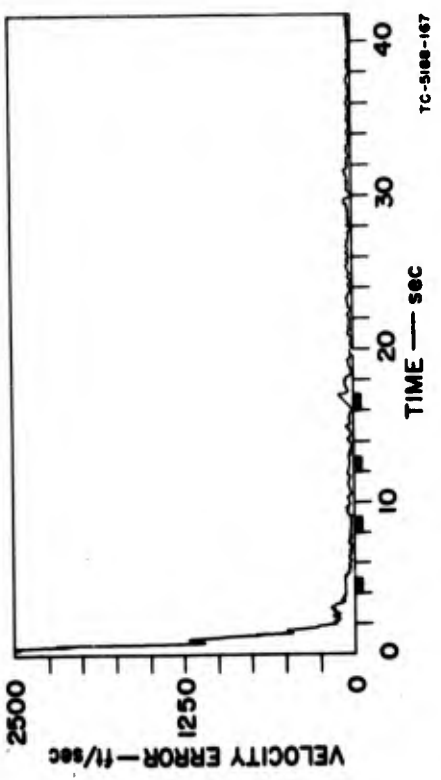


(c)

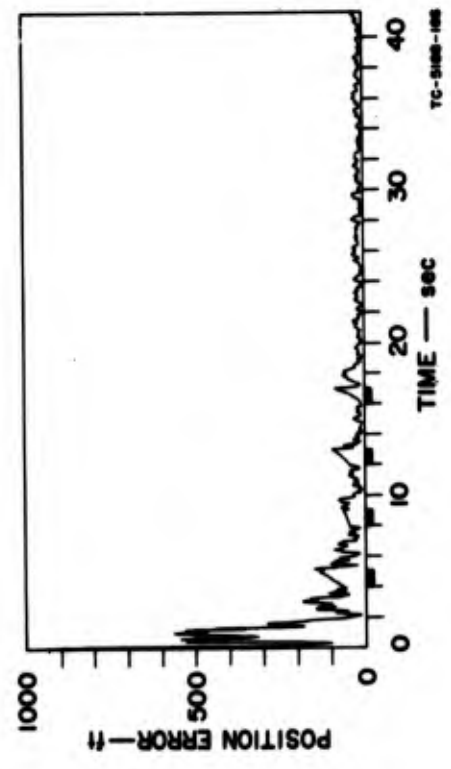


(d)

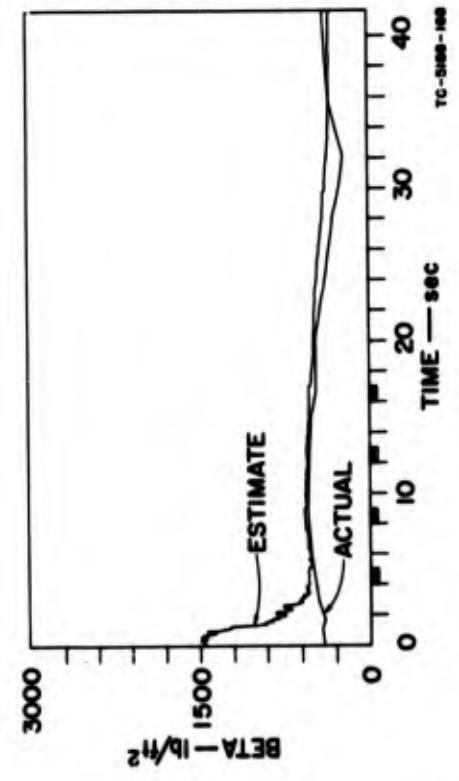
FIG. 17 EFFECT OF DATA INTERRUPTION ON EXTENDED KALMAN FILTER — CASE 1  
(Intervals of data interruption are indicated by bars on time axis.)



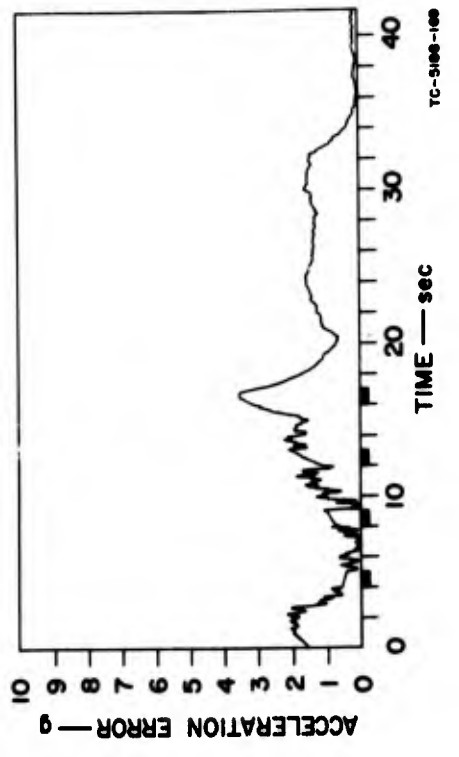
(a)



(b)



(c)



(d)

FIG. 18 EFFECT OF DATA INTERRUPTION ON EXTENDED KALMAN FILTER — CASE 4  
(Intervals of data interruption are indicated by bars on time axis.)

Filter performance during data interruption and subsequent recovery is excellent in both cases, except in one instance where the interruption occurred before the state estimate had begun to converge. Additional errors due to the interruption are within 300 ft, 140 ft/sec, and 1g in the magnitudes of position, velocity, and acceleration, respectively. The additional error in the  $\beta$  estimate is within 150 lb/ft<sup>2</sup>. Recovery after data becomes available again takes place well within 0.5 sec in all cases. The results show that the filter is best able to tolerate a data interruption after it has received sufficient measurements to develop a reasonably good state estimate; late in a run, an interruption of reasonable length will have virtually no effect on performance.

## VII PRECOMPUTATION OF THE WEIGHTING MATRIX

### A. Computational Requirements of the Extended Kalman Filter

Because of the excellent performance of the extended Kalman filter, much interest has been expressed in using it for real-time estimation. However, its computational requirements are so large that this is a difficult task for computers available today. For a data rate of 20 measurements per second, the extended Kalman filter runs approximately six times slower than real time on the IBM 7090—i.e., it takes six seconds of computer time to process the measurements obtained in one second.

In terms of storage requirements, the program as presently written requires approximately 620 locations. For each vehicle being tracked, seven storage locations are required for the last predicted state,  $\hat{x}(k/k - 1)$ , and 28 locations are required for the nonredundant elements of the last (symmetric) predicted covariance matrix  $S(k/k - 1)$ . In order to track 50 vehicles, about 2370 storage locations would be required, a large but manageable number.

Time and storage requirements could be reduced by going to a larger and/or faster computer and by writing a more efficient program. However, these numbers reflect to within an order of magnitude the computer requirements if a present-day, general-purpose computer is used.

### B. Use of a Precomputed Weighting Matrix

One approach to reducing these computational requirements is to precompute  $W(k)$ , the filter weighting matrix. In the case of linear dynamical equations, where  $\Phi(k)$  and  $H(k)$  are known functions of time, the covariance matrices  $S(k/k - 1)$  and  $S(k/k)$ , and hence the weighting matrix  $W(k)$ , can indeed be precomputed. However, in the extended Kalman filter,  $\Phi(k)$  and  $H(k)$  require linearizations about  $\hat{x}(k/k)$  and  $\hat{x}(k/k - 1)$ , respectively. Since these estimates are not known *a priori*, the weighting matrix  $W(k)$  cannot be exactly precomputed.

In experimental computer runs with the extended Kalman filter, it was observed that for the four cases described in Sec. IV the components of

the weighting matrix, as functions of altitude, varied little from case to case. Since the performance of the Kalman filter is relatively insensitive to changes in the weighting matrix, it is reasonable to expect that comparable performance can be achieved by using a precomputed approximation to the weighting matrix. This approximation was computed by using a simple fit to each of the components of the weighting matrix, based on the values obtained in the four cases. The results obtained are discussed in Sec. VII-C. A more elaborate approximation scheme may be expected to yield better results.

The savings in computational requirements obtained by using the precomputed approximation to the weighting matrix are considerable. The only equations that need to be implemented in real time are the vector prediction equation (15) and the vector correction equation (5), where  $W(k)$  is obtained by using the precomputed weighting matrix evaluated as a function of  $\hat{x}_3(k/k - 1)$ , the predicted altitude at time  $k$ . The matrix equations for the covariances  $S(k/k - 1)$  and  $S(k/k)$  need not be implemented.

Experimentally, the computation time using the precomputed approximation to the weighting matrix is a factor of about 30 less than that for the fully implemented extended Kalman filter.\* In terms of storage requirements, the program requires about 240 storage locations, and only the seven components of  $\hat{x}(k/k)$  need to be stored in the high-speed memory in order to compute  $\hat{x}(k + 1/k + 1)$ . The total amount of storage for tracking 50 targets is only about 590 locations. Both time and storage requirements are about the same as for the second-order polynomial filter discussed in Sec. V.

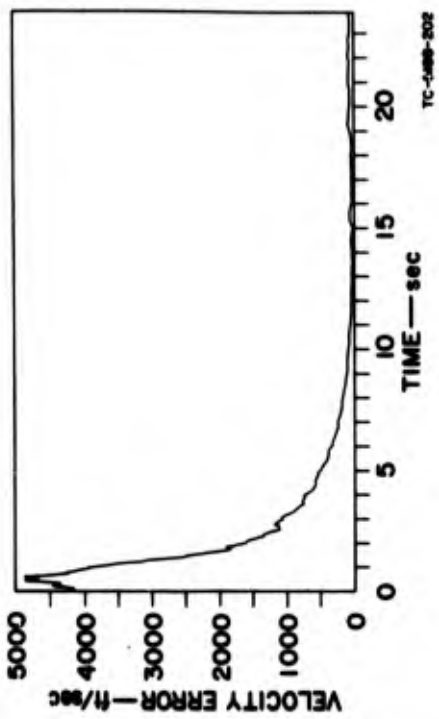
### C. Experimental Results Using a Precomputed Weighting Matrix

The elements of the  $7 \times 3$  weighting matrix fall into two categories. Elements in the first six rows are characterized by a fairly short-lived transient from an initial point to a steady-state constant value as the run progresses. Except at low altitudes, where dependence on the ballistic parameter  $\beta$  is evident, these elements vary little over cases starting at similar altitudes. The elements in the last row, which correct the state  $x_7 = \rho/\beta$ , constitute the second category. The behavior of these elements is essentially exponential as a function of altitude, with the coefficient of altitude in the exponent depending only on altitude. There is only slight variation of these elements over cases starting at similar altitudes. This exponential behavior results from the exponential nature of the atmosphere density  $\rho$ .

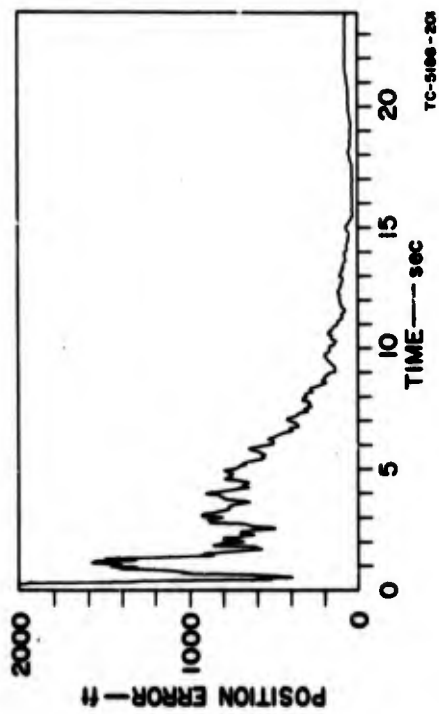
\* This estimate was made from the observation that 1000 iterations of the filter equations required 10 sec on the IEM 7090 using FORTRAN IV.

The approximate weighting matrix then has components that are either piecewise constant or piecewise exponential, after a transient segment determined from the actual weighting matrices of a number of representative cases. More elaborate approximations are possible in order to obtain improved performance.

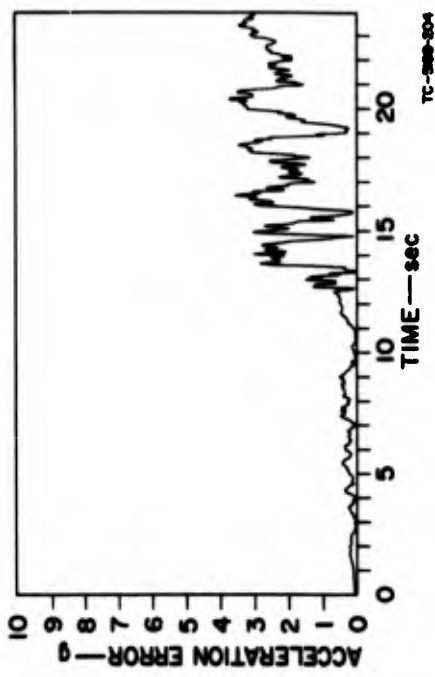
An approximation based on the four cases discussed in Sec. IV was obtained by fitting on the basis of a least-mean absolute criterion. This approximation was found to perform well on all four cases. The results for Cases 1 and 4 are presented in Figs. 19 and 20. As can be seen from Figs. 5, 8, 9, and 12, performance of the precomputed filter is only slightly worse than the fully implemented filter and significantly better than the polynomial filter.



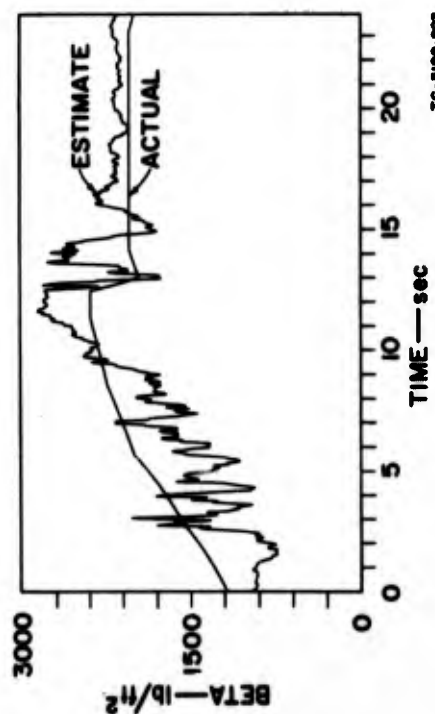
(a)



(b)



(c)



(d)

FIG. 19 PRECOMPUTED FILTER — CASE 1

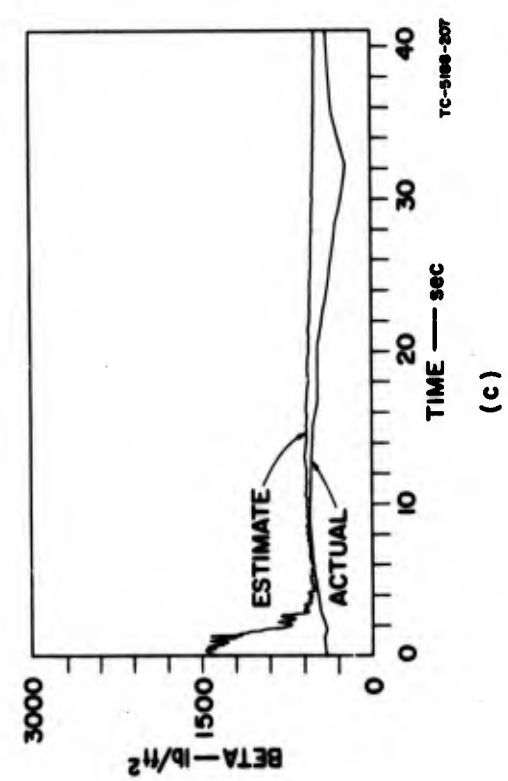
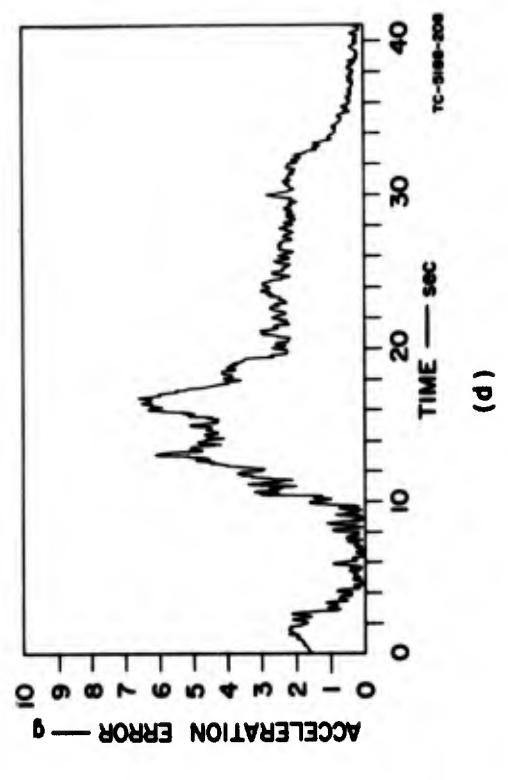
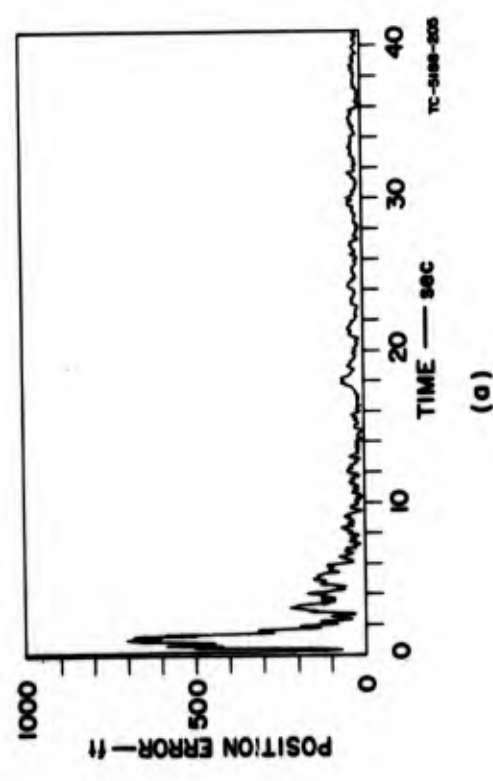
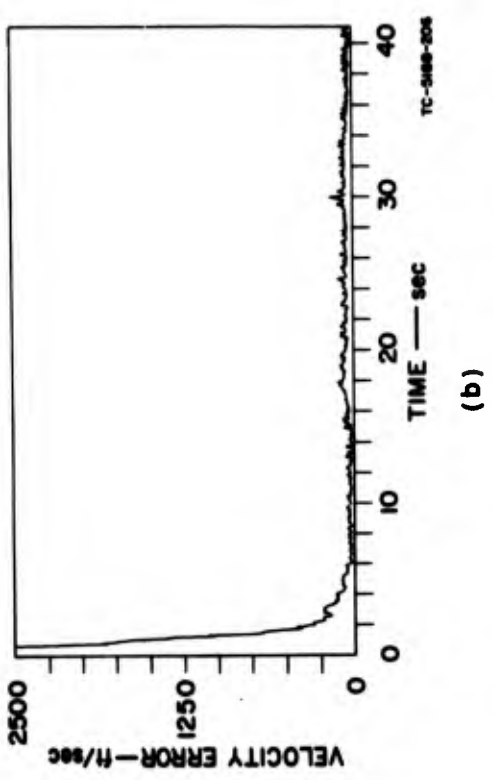


FIG. 20 PRECOMPUTED FILTER — CASE 4

## VIII CONCLUSIONS AND RECOMMENDATIONS FOR FUTURE STUDY

The major conclusion of this study is that the extended Kalman filter is an extremely effective tool for estimation of ballistic trajectories. The filter was tested on several examples, and in all cases results were excellent. The performance was significantly better than for a polynomial filter. Decreasing the data rate by a factor of 5 and introducing multiple one-second blackouts had little effect. Use of a precomputed weighting matrix based on previous runs greatly reduced the computational requirements of the filter at a small cost in filter performance.

One of the most promising areas for future extensions of this work is precomputation of the weighting matrix. The results obtained so far are very encouraging. What remains to be done is to test this filter against more cases and to modify the design parameters if required. A tested and proven filter of this type would be a strong candidate for implementation in the actual NIKE-X system.

If the performance of the precomputed filter is not satisfactory, it is still possible to use a precomputed filter over certain altitude regions. A varying data rate could also be used; for example, a good filter design might be obtained by using the maximum data rate over the initial transient, switching to a much lower data rate for a few seconds, and then using the precomputed weighting matrix for the remainder of the trajectory. A combination filter of this type would have superior performance to the fully precomputed filter, with only a small increase in computational requirements.

Another area for future work is the development of an extended Kalman filter for processing real data. Although the target and radar noise simulations are good approximations to the physical systems, complete confidence in the filter can be gained only after testing it on actual data. A filter for operating on real data, including exoatmospheric portions of the trajectory, is now being programmed.

Still another area for future work is estimation of trajectories for maneuvering re-entry vehicles (MRV). Recent studies of the MRV problem

indicate that such a filter is a vital part of any defensive system.<sup>6</sup> Some experience with a filter to estimate lift parameters as well as  $\beta$  has already been gained by Douglas Aircraft personnel.<sup>7</sup> A filter similar to theirs is now being programmed.

Finally, a task vital to the successful application of this work is the integration of the filter with the functions of identification, prediction, prelaunch, and guidance. This problem has been explored in past reports,<sup>1,8</sup> but further work remains to be done. The filter obtains estimates of  $\beta$ , and presumably will be capable of estimating lift parameters as well, but insufficient attention has been devoted to utilizing these estimates for discrimination and identification. Some work has been done using analytic prediction based on estimated values of position, velocity, and  $\beta$ .<sup>2</sup> The results are very encouraging, but it is not known to what extent prediction can be improved by using a more sophisticated approach. The information the filter generates about the uncertainty of the estimates—namely, the covariance matrices  $S(k/k - 1)$  and  $S(k/k)$ —could be used to upgrade both the prelaunch and guidance routines; a conceptual framework for achieving this is given in Ref. 8, but little has been done toward implementation. Only by utilizing the best available techniques in all of these areas and interfacing them properly can an overall system capable of a true evaluation be designed.

## REFERENCES

1. J. Peschon and R. E. Larson, "Analysis of an Intercept System," Final Report, SRI Project 5188-7, Contract DA-01-021-AMC-90006(Y), Stanford Research Institute, Menlo Park, California (December 1965).
2. G. McGlone, "Comparison of the Accuracy of the Kalman-Bucy and Second-Order Filters," Research Memorandum 254, Stanford Research Institute, Huntsville, Alabama (October 1966).
3. J. P. McHenry and P. K. Whalen, "NIKE-X MSR Error Equations (U)," Technical Note SED 140, Stanford Research Institute, Menlo Park, California (September 1966) SECRET.
4. R. E. Kalman, "A New Approach to Linear Filtering and Prediction Problems," *Trans. ASME, J. Basic Engr.*, pp. 35-45 (March 1960).
5. R. M. Dressler, "Analysis of a Recursive Smoothing Technique," Technical Memorandum 19, SRI Project 5188-103, Contract DA-01-021-AMC-90006(Y), Stanford Research Institute, Menlo Park, California (July 1966).
6. R. E. Larson, "An Initial Differential Games Approach to Target Interception," Technical Memorandum 21, SRI Project 5188-103, Contract DA-01-021-AMC-90006(Y), Stanford Research Institute, Menlo Park, California (September 1966).
7. R. A. Hinker, "MRV Tracking Simulation," Internal Memorandum A2-260-AA2-ZN6462, Douglas Aircraft Company, Santa Monica, California (11 October 1966).
8. R. E. Larson, "Optimum Guidance Laws for an AMM," Preliminary Report, SRI Project 5188-7, Contract DA-01-021-AMC-90006(Y), Stanford Research Institute, Menlo Park, California (January 1966).
9. R. S. Ratner, "Noise Model of NIKE-X MSR for Implementation in Extended Kalman Filter (U)," Technical Memorandum 22, SRI Project 5188-203, Contract DA-01-021-AMC-90006(Y), Stanford Research Institute, Menlo Park, California (February 1967) SECRET.

UNCLASSIFIED

Security Classification

DOCUMENT CONTROL DATA - R&D

(Security classification of title, body of abstract and indexing annotation must be entered when the overall report is classified)

1. ORIGINATING ACTIVITY (Corporate author) Stanford Research Institute Menlo Park, California	2a. REPORT SECURITY CLASSIFICATION UNCLASSIFIED
	2b. GROUP N/A

3. REPORT TITLE  
APPLICATION OF THE EXTENDED KALMAN FILTER TO BALLISTIC TRAJECTORY ESTIMATION

4. DESCRIPTIVE NOTES (Type of report and inclusive dates)  
Final Report covering the Period 1 October 1965 to 30 September 1966

5. AUTHOR(S) (Last name, first name, initial)  
Larson, Robert E.; Dressler, Robert M.; Ratner, Robert S.

6. REPORT DATE January 1967	7a. TOTAL NO. OF PAGES 53	7b. NO. OF REFS 9
--------------------------------	------------------------------	----------------------

8a. CONTRACT OR GRANT NO. Contract DA-01-021-AMC-90006(Y) <i>revised</i>	9a. ORIGINATOR'S REPORT NUMBER(S) Final Report Project 5188-103
b. PROJECT NO.	
c.	9b. OTHER REPORT NO(S) (Any other numbers that may be assigned this report)
d.	

10. AVAILABILITY/LIMITATION NOTICES

11. SUPPLEMENTARY NOTES	12. SPONSORING MILITARY ACTIVITY Nike-X Project Office U.S. Army Materiel Command Redstone Arsenal, Alabama
-------------------------	--

13. ABSTRACT

↙ In this report an extended Kalman filter for ballistic trajectory estimation is presented. The filter equations are basically the same as those in the previous Final Report on this contract. The several modifications are explained in detail, and values for all filter parameters are given. The filter was tested against simulated radar data for a number of different cases; performance was excellent in all cases. For comparison purposes a second-order exponentially weighted polynomial filter was used on the same data; the performance was significantly worse than for the extended Kalman filter. The extended Kalman filter was also run at slower data rates and with multiple interruptions of data with only a slight degradation in performance. A precomputed approximation to the weighting matrix was calculated on the basis of several runs; this approximation performed nearly as well as the fully implemented filter. Use of this approximation reduced computational requirements by an order of magnitude. ↗

## Security Classification

14. KEY WORDS	LINK A		LINK B		LINK C	
	ROLE	WT	ROLE	WT	ROLE	WT
Ballistic trajectory estimation Kalman filter Filter comparisons						

## INSTRUCTIONS

1. **ORIGINATING ACTIVITY:** Enter the name and address of the contractor, subcontractor, grantee, Department of Defense activity or other organization (*corporate author*) issuing the report.

2a. **REPORT SECURITY CLASSIFICATION:** Enter the overall security classification of the report. Indicate whether "Restricted Data" is included. Marking is to be in accordance with appropriate security regulations.

2b. **GROUP:** Automatic downgrading is specified in DoD Directive 5200.10 and Armed Forces Industrial Manual. Enter the group number. Also, when applicable, show that optional markings have been used for Group 3 and Group 4 as authorized.

3. **REPORT TITLE:** Enter the complete report title in all capital letters. Titles in all cases should be unclassified. If a meaningful title cannot be selected without classification, show title classification in all capitals in parenthesis immediately following the title.

4. **DESCRIPTIVE NOTES:** If appropriate, enter the type of report, e.g., interim, progress, summary, annual, or final. Give the inclusive dates when a specific reporting period is covered.

5. **AUTHOR(S):** Enter the name(s) of author(s) as shown on or in the report. Enter last name, first name, middle initial. If military, show rank and branch of service. The name of the principal author is an absolute minimum requirement.

6. **REPORT DATE:** Enter the date of the report as day, month, year, or month, year. If more than one date appears on the report, use date of publication.

7a. **TOTAL NUMBER OF PAGES:** The total page count should follow normal pagination procedures, i.e., enter the number of pages containing information.

7b. **NUMBER OF REFERENCES:** Enter the total number of references cited in the report.

8a. **CONTRACT OR GRANT NUMBER:** If appropriate, enter the applicable number of the contract or grant under which the report was written.

8b, 8c, & 8d. **PROJECT NUMBER:** Enter the appropriate military department identification, such as project number, subproject number, system numbers, task number, etc.

9a. **ORIGINATOR'S REPORT NUMBER(S):** Enter the official report number by which the document will be identified and controlled by the originating activity. This number must be unique to this report.

9b. **OTHER REPORT NUMBER(S):** If the report has been assigned any other report numbers (*either by the originator or by the sponsor*), also enter this number(s).

10. **AVAILABILITY/LIMITATION NOTICES:** Enter any limitations on further dissemination of the report, other than those

imposed by security classification, using standard statements such as:

- (1) "Qualified requesters may obtain copies of this report from DDC."
- (2) "Foreign announcement and dissemination of this report by DDC is not authorized."
- (3) "U. S. Government agencies may obtain copies of this report directly from DDC. Other qualified DDC users shall request through \_\_\_\_\_."
- (4) "U. S. military agencies may obtain copies of this report directly from DDC. Other qualified users shall request through \_\_\_\_\_."
- (5) "All distribution of this report is controlled. Qualified DDC users shall request through \_\_\_\_\_."

If the report has been furnished to the Office of Technical Services, Department of Commerce, for sale to the public, indicate this fact and enter the price, if known.

11. **SUPPLEMENTARY NOTES:** Use for additional explanatory notes.

12. **SPONSORING MILITARY ACTIVITY:** Enter the name of the departmental project office or laboratory sponsoring (*paying for*) the research and development. Include address.

13. **ABSTRACT:** Enter an abstract giving a brief and factual summary of the document indicative of the report, even though it may also appear elsewhere in the body of the technical report. If additional space is required, a continuation sheet shall be attached.

It is highly desirable that the abstract of classified reports be unclassified. Each paragraph of the abstract shall end with an indication of the military security classification of the information in the paragraph, represented as (TS), (S), (C), or (U).

There is no limitation on the length of the abstract. However, the suggested length is from 150 to 225 words.

14. **KEY WORDS:** Key words are technically meaningful terms or short phrases that characterize a report and may be used as index entries for cataloging the report. Key words must be selected so that no security classification is required. Identifiers, such as equipment model designation, trade name, military project code name, geographic location, may be used as key words but will be followed by an indication of technical context. The assignment of links, roles, and weights is optional.